Bioorganic Chemistry 105 (2020) 104399

Contents lists available at ScienceDirect

Bioorganic Chemistry

journal homepage: www.elsevier.com/locate/bioorg

Design, synthesis, molecular docking and anti-proliferative evaluations of [1,2,4]triazolo[4,3-*a*]quinoxaline derivatives as DNA intercalators and Topoisomerase II inhibitors

Khaled El-Adl [a,b,*], Abdel-Ghany A. El-Helby [a], Helmy Sakr [a], Alaa Elwan [a,*]

[a] Pharmaceutical Medicinal Chemistry and Drug Design Department, Faculty of Pharmacy (Boys), Al-Azhar University, Nasr City 11884, Cairo, Egypt
[b] Pharmaceutical Chemistry Department, Faculty of Pharmacy, Heliopolis University for Sustainable Development, Cairo, Egypt

ARTICLE INFO

Keywords:
[1,2,4]Triazolo[4,3-*a*]quinoxaline
Molecular docking
DNA intercalators
Top II inhibitors
Anticancer agents

ABSTRACT

In view of their DNA intercalation activities as anticancer agents, novel twenty four [1,2,4]triazolo[4,3-*a*]quinoxaline derivatives have been designed, synthesized and evaluated against HepG2, HCT-116 and MCF-7 as DNA intercalators and Top II enzyme inhibitors. The data obtained from molecular modeling studies revealed that, our small aromatic molecules were concluded to act through two ways firstly, through non-covalent interaction with the directly bound proteins to DNA hence inhibit topoisomerase-II enzyme. The second is through non-covalently binding to double helical structures of DNA either by intercalating binder as in compounds **10$_a$** and **11$_d$** or by minor groove binding as in compounds **8$_e$** and **8$_c$**. Cytotoxic activity indicated that MCF-7 and HepG2 were the most sensitive cell lines to the influence of the new derivatives respectively. In particular, compounds **10$_a$**, **11$_d$** and **8$_e$** were found to be the most potent derivatives overall the tested compounds against the three HepG2, HCT116 and MCF-7 cancer cell lines with IC_{50} = (4.55 ± 0.3, 6.18 ± 0.8 and 3.93 ± 0.6 μM), (5.61 ± 0.5, 6.49 ± 0.5and 3.71 ± 0.3 μM) and (4.66 ± 0.3, 8.08 ± 0.8 and 5.11 ± 0.7 μM) respectively. The three derivatives exhibited higher activities than **doxorubicin**, (IC_{50} = 7.94 ± 0.6, 8.07 ± 0.8 and 6.75 ± 0.4 μM respectively), against HepG2 and MCF-7 but **8$_e$** exhibited nearly the same activity against HCT116 cancer cell lines respectively. The most active derivatives **8$_{a-e}$**, **10$_{a,b}$**, **11$_{b-e}$**, **13$_a$** and **14$_{b,c}$** were evaluated for their DNA binding activities. The tested compounds displayed very good to moderate DNA-binding affinities. Compounds **10$_a$** **11$_d$**, **8$_e$**, **8$_c$**, **8$_a$** and **8$_b$** displayed the highest binding affinities. These compounds potently intercalate DNA at decreased IC_{50} values of 25.27 ± 1.2, 27.47 ± 2.1, 27.54 ± 3.2, 27.78 ± 1.3, 29.15 ± 1.8 and 30.23 ± 3.7 μM respectively, which were less than that of doxorubicin (31.27 ± 1.8). Furthermore, the most active cytotoxic compounds **8$_a$**, **8$_b$**, **8$_c$**, **8$_e$**, **10$_a$** and **11$_d$** were selected to evaluate their inhibitory activities against Topo II enzyme. All the tested compounds could interfere with the Topo II activity. They exhibited very good inhibitory activities with IC_{50} values ranging from 0.379 ± 0.07 to 0.813 ± 0.14 μM that were lower than that of doxorubicin (IC_{50} = 0.94 ± 0.4 μM). For a great extent, the reported results were in agreement with that of *in vitro* cytotoxicity activity, DNA binding and molecular modeling studies.

1. Introduction

One of the most clinically useful anticancer drugs are DNA intercalators targeting Topoisomerase II as inhibitors and are normally referred to Topo II poisons because they convert the Topo II enzyme into a DNA-damaging agent [1–3]. Extensive research over the last four decades has focused on the small organic compounds effects that non-covalently bind to nucleic acids [4]. These interactions are known to disrupt replication and/or transcription that culminate in cellular death. Accordingly, DNA-binding compounds have potential applications as anticancer agents. Small molecules may bind noncovalently to DNA through intercalation between nucleobase pairs, major or minor groove binding and electrostatic interactions [5].

There are three principally different ways of anticancer drug binding. First is through control of transcription factors and polymerases. Here, the anticancer drugs interact with the directly bound proteins to

* Corresponding authors at: Pharmaceutical Medicinal Chemistry and Drug Design Department, Faculty of Pharmacy (Boys), Al-Azhar University, Nasr City 11884, Cairo, Egypt (K. El-Adl).
E-mail addresses: eladlkhaled74@yahoo.com, eladlkhaled74@azhar.edu.eg, khaled.eladl@hu.edu.eg (K. El-Adl), alaaelwan34@gmail.com (A. Elwan).

https://doi.org/10.1016/j.bioorg.2020.104399
Received 26 June 2020; Received in revised form 27 September 2020; Accepted 17 October 2020
Available online 21 October 2020

DNA. Second is through RNA binding to the double helices of DNA to form triple helical structures of nucleic acid or RNA hybridization to the single strand regions of exposed DNA to form DNA-RNA hybrids which may interfere with transcriptional activity. Third is through small aromatic molecules that non-covalently bind to double helical structures of DNA either by intercalating binder or by minor groove binders (Fig. 1) [6,7].

So compounds have planar aromatic systems (known as chromophores) are inserted between adjacent base pairs of the DNA helix perpendicularly to its axis forming strong non-covalent interactions with DNA bases [8,9]. This complex between drug and DNA deforms and uncoils the DNA [8], also the structural changes induced in DNA by intercalation lead to interference with recognition and function of DNA associated proteins or enzymes involved in replication, transcription processes, and DNA repair systems (especially topoisomerases) inhibiting the functions of this enzymes leading to failure of this processes [8].

In addition, the binding of intercalators involves the insertion of a planar aromatic molecule between DNA base pairs, which results in a decrease in the DNA helical twist and lengthening of the DNA. While groove binding, unlike intercalation, does not induce large conformational changes in DNA and may be considered similar to standard lock-and-key models for ligand-macromolecular binding. In addition, Groove binders are usually crescent-shaped molecules that bind to the minor groove of DNA [7].

There are two major types of topoisomerases. i)Topoisomerase I (Topo I), which cleaves one strand of a DNA duplex, relax the strand, and resealing the strand. ii) Topoisomerase II (Topo II), which cleaves both strands of the DNA helix simultaneously in order to remove DNA supercoiling [10].These enzymes covalently bind to the DNA via tyrosine residues in the active site. These linkages are transient and easily reversible. So that, the covalently bound structure is known as the cleavable complex [11]. Accordingly, topoisomerases are considered as prevalent targets for cancer chemotherapy treatments [2], as topoisomerase inhibitors block the ligation step of the cell cycle, generating single and double stranded breaks that harm the integrity of the genome [12].

Anticancer drugs targeting Topo II inhibit the enzymatic activity as a primary mode of action, and are known as ‘catalytic Topo II inhibitors [13]. Another type of Topo II targeting drugs, including intercalating drugs, interfere with the enzyme’s cleavage and rejoining activities by trapping the cleavable complex and thereby increasing the half- life of the transient Topo II catalyzed DNA breaks. Some of the most clinically useful anticancer drugs are from the latter type and are normally referred to Topo II poisons because they convert the Topo II enzyme into a DNA-damaging agent [2,13]. DNA intercalators as Topo II poisons are molecules that intercalate between DNA base pairs. They have attracted particular attention due to their promising antitumor activities [14]. Many intercalative Topo II poisons are either used already as anticancer drugs or still under clinical trials (e.g., doxorubicin **I** [15], amsacrine **II** [16], mitoxantrone **III** [17] ellipticine **IV** [18] nogalamycin **V** [19]) (Fig. 2).

Quinoxaline nucleus is the backbone of many DNA intercalators and Topoisomerase II inhibitors [20–23]. The discovery and development of new therapeutic DNA intercalators for the treatment of cancer is considered as one of the most important targets in the field of medicinal chemistry [24]. Quinoxaline analogues prohibited excellent anticancer activities through DNA intercalation, for instance, echinomycin **VI**, a natural DNA intercalator, showed potent activities in phase I and II trials against a wide array of cancer [25]. Moreover, N^3-(3-(dimethylamino) propyl)-N^2-(4-methoxybenzyl)-6-nitroquinoxaline-2,3-diamine **VII** is of current interest in view of its binding to DNA [26].

Based on the earlier findings, and in continuation of our previous research in design and synthesis of new anticancer agents [27–33], especially Topo II inhibitors and DNA intercalators [20], we reported the design, synthesis, DNA binding examination and docking studies of a new series of quinoxaline derivatives. These derivatives were designed according to the main pharmacophoric features of DNA intercalators.

1.1. *Rationale and structure-based design*

DNA intercalators and Topo II poisons share three common essential structural features, i) a planar polyaromatic system involves fused planar rings (chromophore), binding with DNA [34,35]. ii) Cationic species which increase the efficiency of DNA intercalators by interaction with the negatively charged DNA sugar–phosphate backbone. The cationic species are basic groups (ex: amino or nitrogen containing

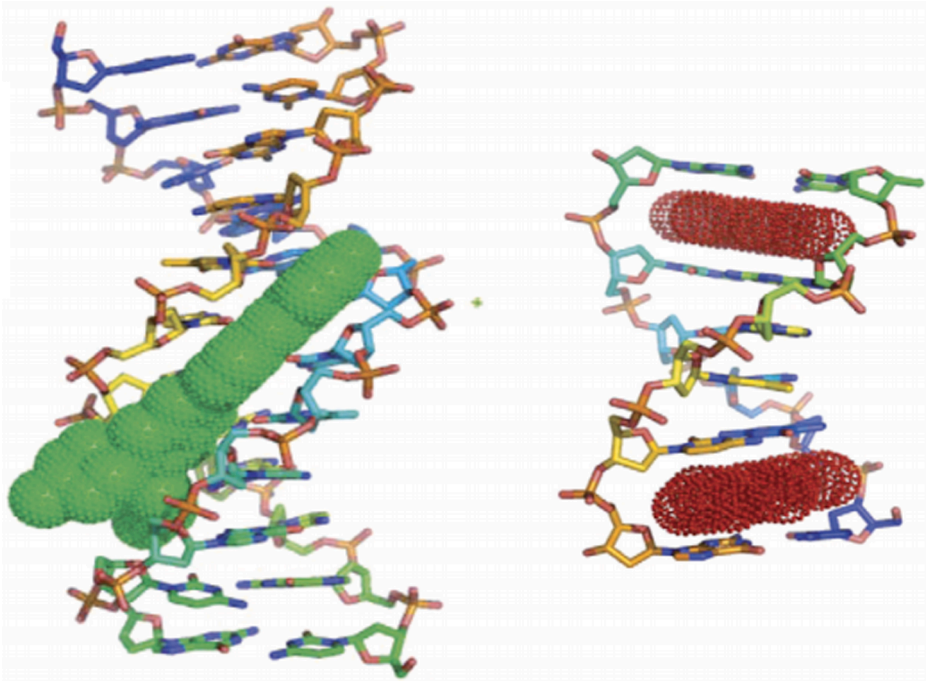

Fig. 1. Groove binding to the minor groove of DNA (left) and the intercalation into DNA (right).

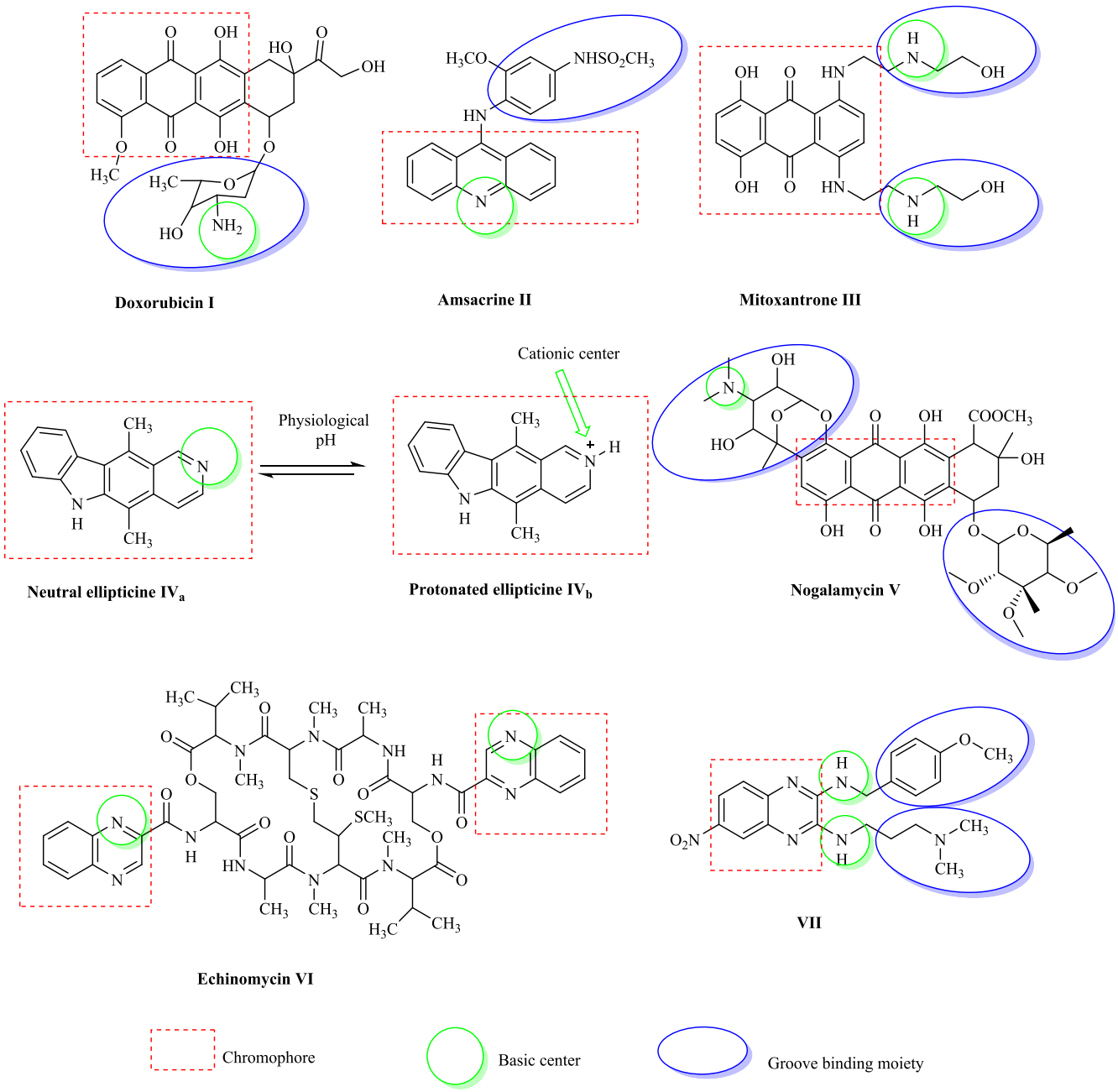

Fig. 2. Some reported DNA intercalators and their basic pharmacophoric features.

heterocyclic groups) that can be protonated under physiological pH [18]. iii) Groove binding side chain, which can occupy the minor groove of DNA [36–38] (Fig. 2).

The rationale of our molecular design depended on molecular hybridization of quinoxaline moiety with triazoles, ester, alkylamino, acid hydrazide, semicarbazides, thiosemicarbazides, pyrazoles, sulfonamides sulfonylurea and/or sulfonylthiourea derivatives to produce [1,2,4]triazolo [4,3-a]quinoxaline scaffold as chromophore attached to a groove binding side chain at position-4 to act as classical DNA intercalators. The choice of the different substituents was based on their relatively high lipophilicity to pass the nuclear membranes aiming to have a strong DNA intercalation. Moreover, the variability of substitutions enabled us to study structure-activity relationship of the final compounds (Fig. 3).

In general, the designed compounds were synthesized and evaluated for their *in vitro* antiproliferative activities against three human tumor cell lines, namely, hepatocellular carcinoma (HCC) type (HepG2), human colorectal carcinoma-116 (HCT-116) and breast cancer (michigan cancer foundation-7 (MCF-7)). The results prompted us to carry out further examinations to reach a deep insight about the mechanism of action of the synthesized compounds.

Firstly, the most cytotoxic agents were further evaluated to assess their binding affinities against DNA through DNA/methyl green assay. Secondly, the highly potent derivatives were further tested as Topo II inhibitors. Finally, a molecular docking was carried out to examine the binding patterns with the prospective target, DNA-Topo II complex (PDB-code: 3qx3).

2. Results and discussion

2.1. Chemistry

For synthesis of the target compounds, the sequence of the reactions

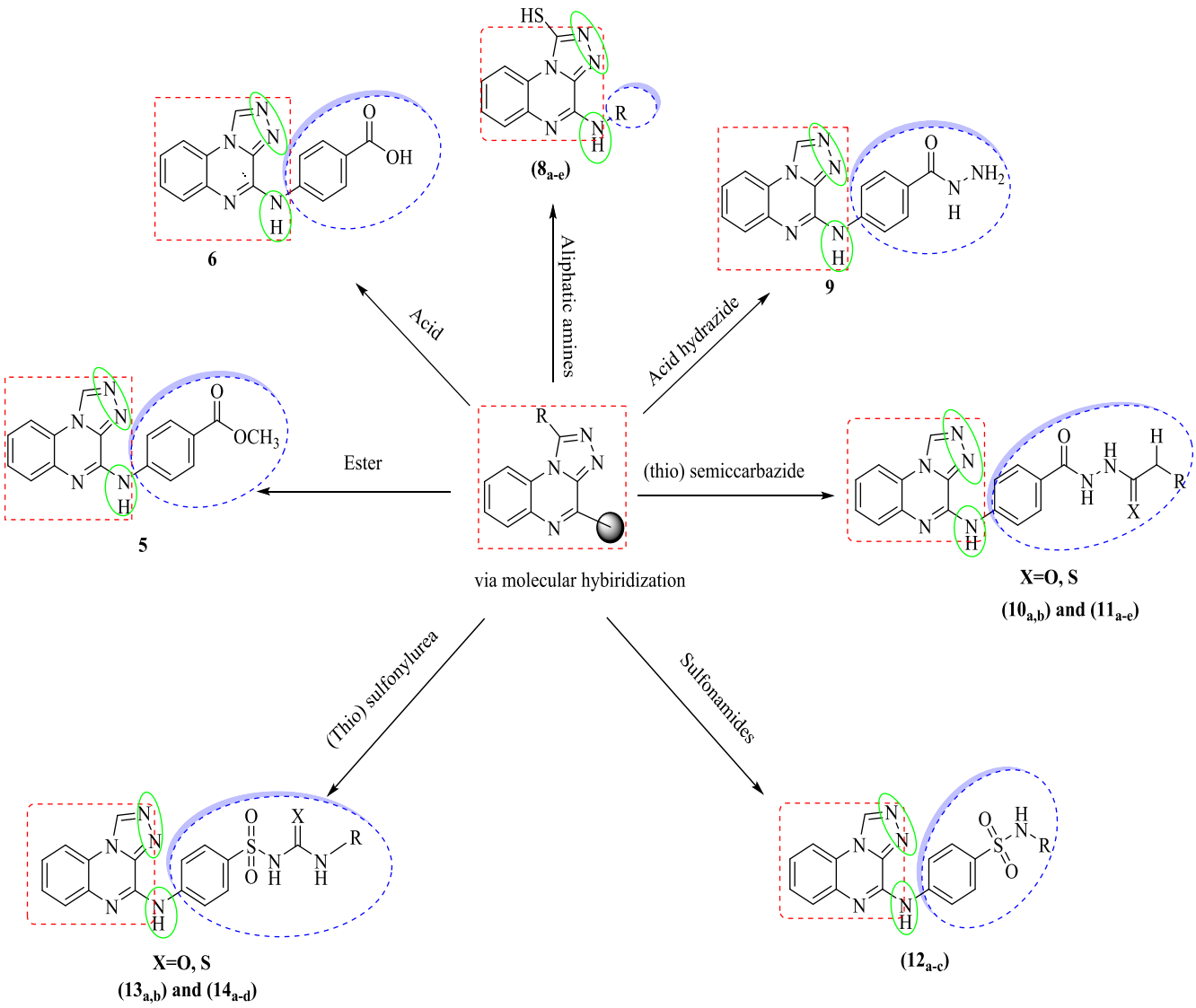

Fig. 3. Rationale of molecular design of new DNA-intercalators.

is illustrated in Schemes 1–3 *o*-Phenylenediamine reacted with oxalic acid in the presence of 4 N HCl to give 2,3-(1*H*,4*H*)-quinoxalinedione **1** [21,39]. The latter was treated with thionyl chloride to afford 2,3-dichloroquinoxaline **2** [21,39] which underwent reaction with hyrazine hydrate while continuous stirring at room temperature to produce 2-chloro-3-hydrazinylquinoxaline **3** [21]. Cyclization of **3** with triethylorthoformate resulted in 4-chloro[1,2,4]triazolo[4,3-*a*]quinoxaline **4** [21]. Heating under reflux of **4** with methyl 4-aminobenzoate and/or 4-aminobenzoic acid in acetonitrile afforded the corresponding methyl ester **5** and/or acid **6** derivatives respectively. On the other hand, cyclization of 2,3-dichloroquinoxaline **2** with CS_2 in the presence of KOH in absolute ethanol followed by acidification using diluted HCl afforded the corresponding 4-chloro-[1,2,4]triazolo[4,3-*a*]quinoxaline-1-thiol **(7)** [40] which underwent reactions with the appropriate alkyl amine to afford the corresponding derivatives $\mathbf{8_{a-e}}$ respectively (Scheme 1).

The methyl ester **5** was treated with hydrazine hydrate to obtain the corresponding acid hydrazide **9** which allowed to react with the appropriate isocyanate and/or isothiocyanate to afford the corresponding semicarbazides $\mathbf{10_{a,b}}$ and/or thiosemicarbazides $\mathbf{11_{a-e}}$ respectively (Scheme 2).

Furthermore, heating of **4** with the appropriate 4-aminobenzenesulfonamide derivative in acetonitrile resulted in the corresponding sulfonamide $\mathbf{12_{a-c}}$ derivatives respectively. Finally, the sulfanilamide derivative $\mathbf{12_a}$ was further treated with the appropriate isocyanate and/or isothiocyanate in dry acetone in the presence of K_2CO_3 (anhydrous) to produce the corresponding sulfonylurea $\mathbf{13_{a,b}}$ and/or sulfonylthiourea $\mathbf{14_{a,d}}$ respectively (Scheme 3).

2.2. Docking studies

Molecular docking investigational study was performed using Discovery Molsoft software for the synthesized compounds and doxorubicin as a reference DNA intercalator and Topo II inhibitor (DNA-Topo II poisons). This study was carried out in order to gain further insight into the binding modes of the synthesized compounds into the DNA binding site of Topo II (PDB ID: 4G0U) [41]. The binding free energies (ΔG) were presented in Table 1. All studied ligands have similar position and orientation inside the DNA binding site of DNA-Topo II (Fig. 4).

The most favorable pose was selected according to the minimum free energy of the DNA–ligand complex for analyzing the interaction between the ligand and the DNA.

The proposed binding mode of the co-crystallized ligand **amsacrine** revealed affinity value of −101.73 kcal/mol and eight H-bonds. The planar aromatic system occupied the same hydrophobic pocket formed by Phenyalanine834, Phenyalanine738, Glutamine742, Leucine799,

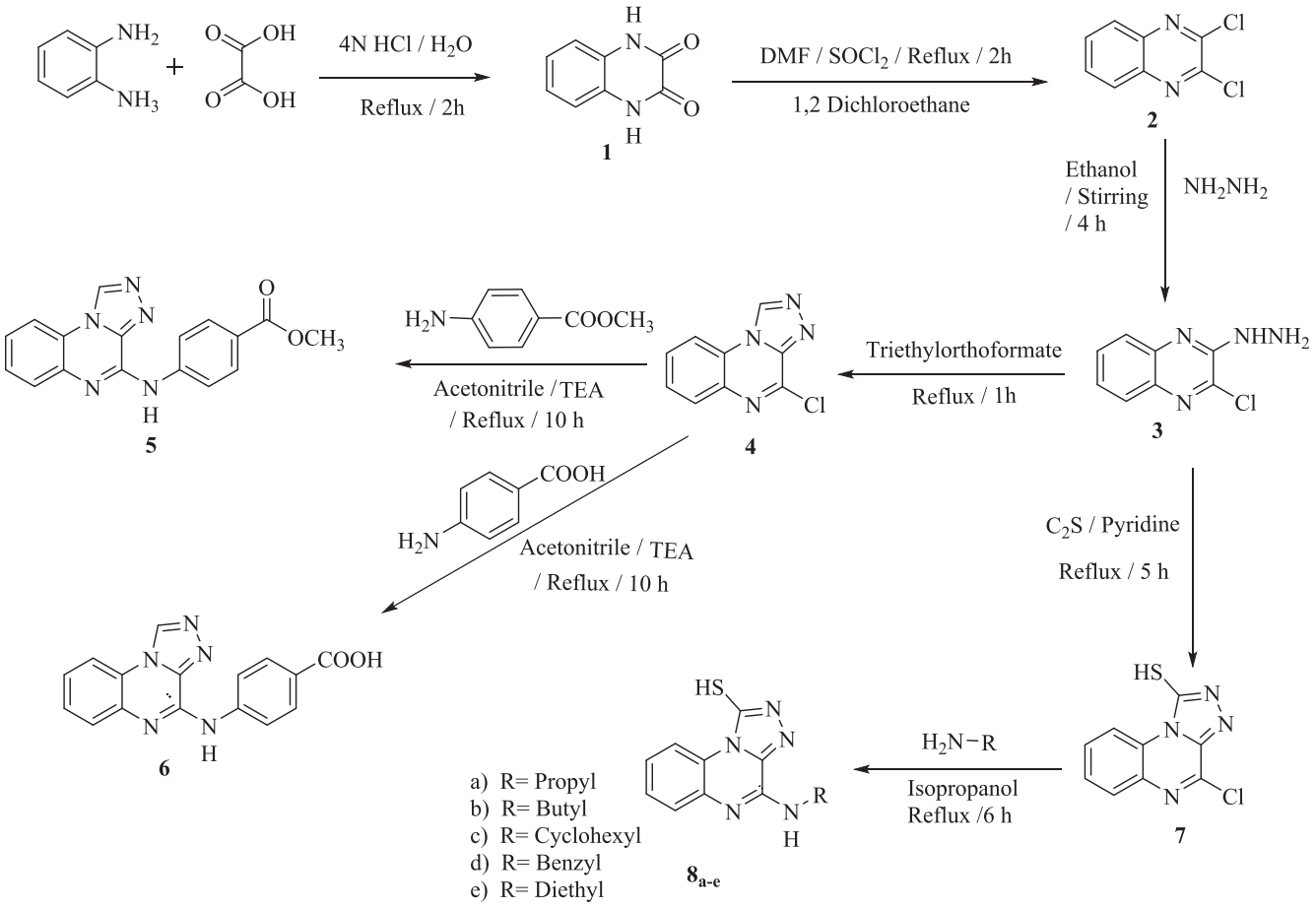

Scheme 1. Synthetic route for preparation of the target compounds **5-8$_{a-e}$**.

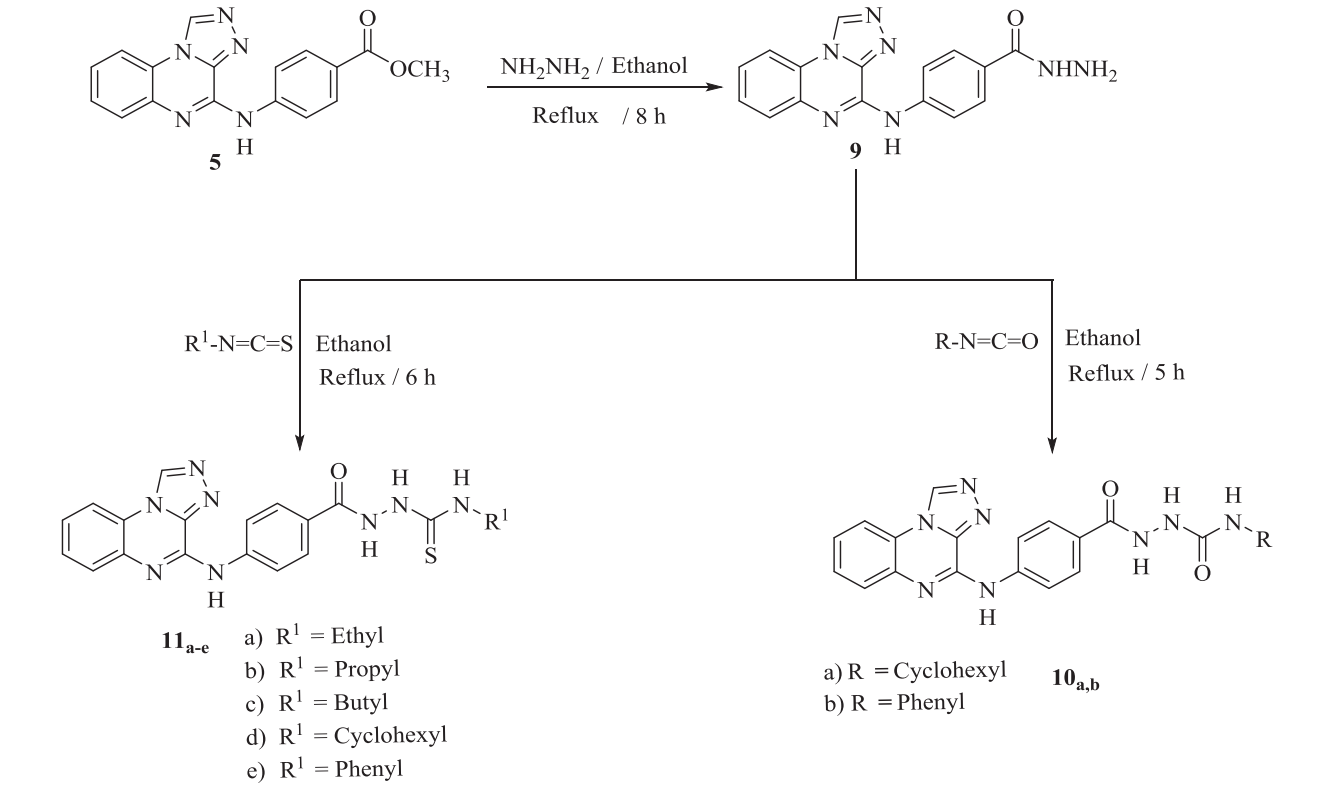

Scheme 2. Synthetic route for preparation of the target compounds **9-11$_{a-e}$**.

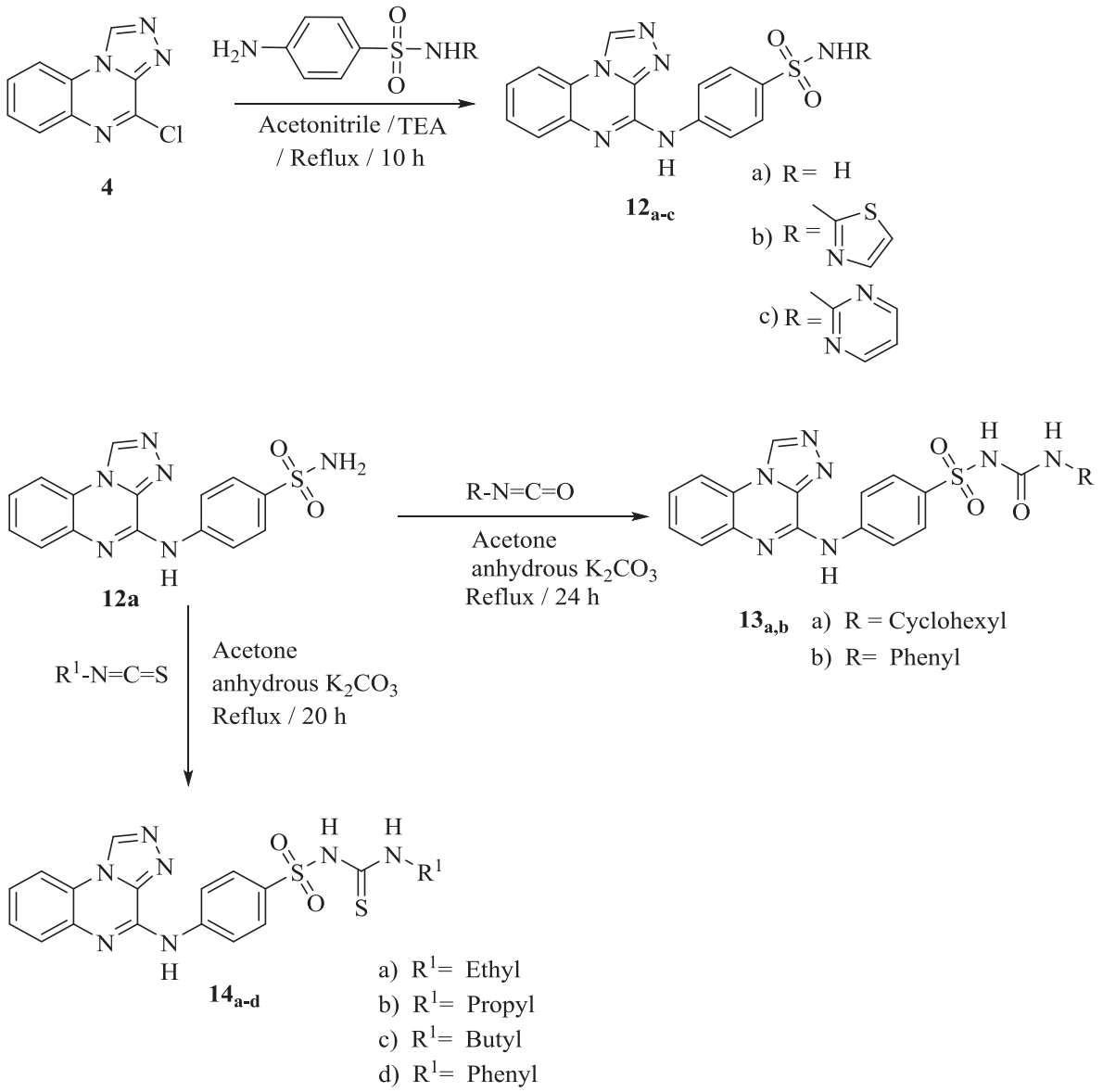

Scheme 3. Synthetic route for preparation of the target compounds **12-14**$_{a\text{-}d}$.

Table 1
The calculated free energy of binding (ΔG in Kcal/mole) for the ligands.

Compound	ΔG [kcal mol^{-1}]	Compound	ΔG [kcal mol^{-1}]
5	−75.91	**11$_d$**	−95.97
6	−74.15	**11$_e$**	−82.33
8$_a$	−86.68	**12$_a$**	−70.55
8$_b$	−86.88	**12$_b$**	−69.82
8$_c$	−87.47	**12$_c$**	−73.29
8$_d$	−78.47	**13$_a$**	−78.99
8$_e$	−88.11	**13$_b$**	−69.87
9	−70.85	**14$_a$**	−74.56
10$_a$	−100.96	**14$_b$**	−80.08
10$_b$	−80.94	**14$_c$**	−80.14
11$_a$	−76.77	**14$_d$**	−75.40
11$_b$	−83.84	**Doxorubicin**	−100.31
11$_c$	−83.77	**Amsacrine**	−101.73

Asparagine798, Arginine1025, Leucine787, Asparagine786, Arginine945, Asparagine867, Asparagine795, Glycine868, Alanine869, Glycine737 and Leucine799. It also stacked between the diphosphate Cytidine (Dc3, Dc4 and Dc8), diphosphate Guanosine (Dg5 Dg10 and Dg13) and Adinine monophosphate 6 (Da6). Its amino group formed one H-bond with Asparagine786. The N-(3-methoxyphenyl)-methanesulfonamide side chain was oriented into minor groove of DNA and stabilized by formation of seven H-bonds with the key amino acids (5H-bonds with Arginine945, one H-bond with Glycine793 and one H-bond with Serine794) (Fig. 5).

The proposed binding mode of **doxorubicin** revealed affinity value of −100.31 kcal/mol and ten H-bonds. The planar aromatic system occupied the hydrophobic pocket formed by Asparagine882, Lucine880, Glutamate870, Alanine869, Glycine868, Asparagine867, Asparagine795, Glutamine789, Asparagine786, Glutamine742, Lysine739, Phenyalanine738 and Glycine737. It formed five H-bonds with the key amino acids in the active site (one H-bond with Asparagine786, two H-bonds with Asparagine795, one H bond with Arginine945, one H-bond with Asparagine867). It also stacked between the diphosphate Cytidine (Dc3, Dc4 and Dc8), diphosphate Guanosine (Dg5, Dg10 and Dg13) and Adinine monophosphate 6 (Da6). The sugar moiety was oriented into minor groove of DNA and stabilized by formation of five H-bonds with the key amino acids (two H-bonds with Arginine945, one H-bonds with Leucine880 and two H-bonds with Asparagine882) (Fig. 6).

The proposed binding mode of **10$_a$** exhibited affinity value of

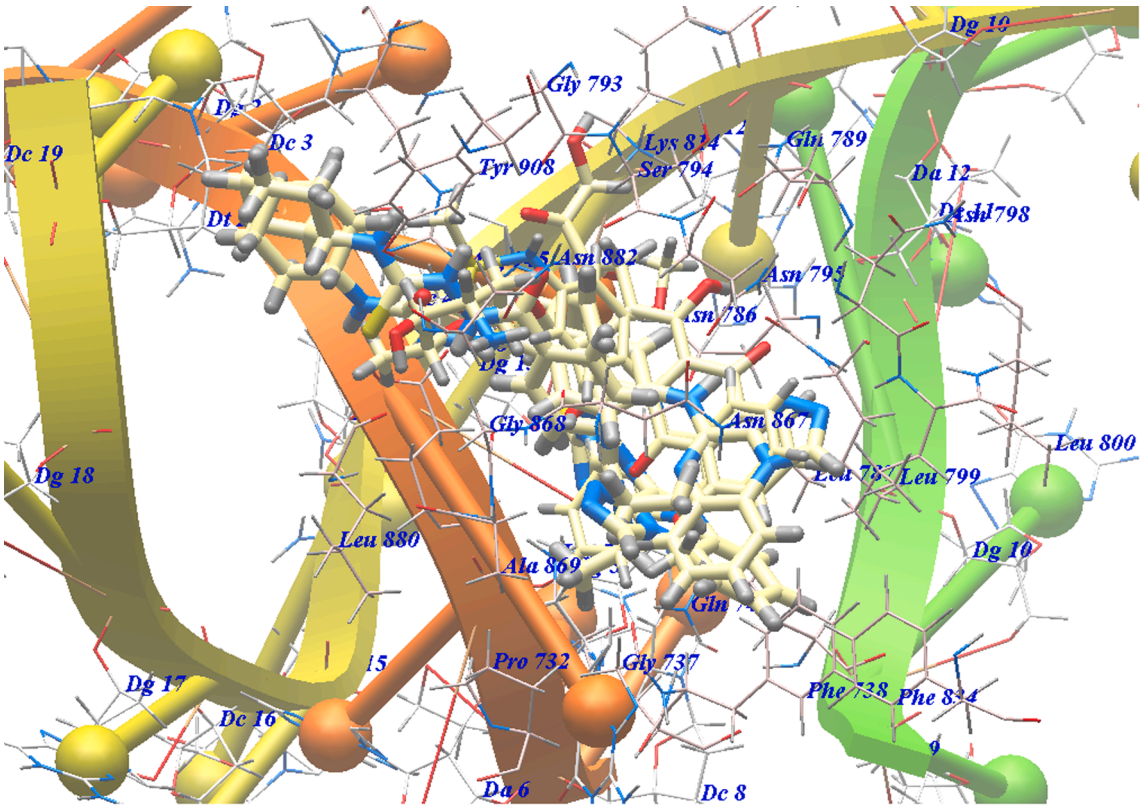

Fig. 4. superimposition of the docked compounds and doxorubicin inside the active site of DNA-Topo II.

−100.96 kcal/mol and seven H-bonds. The planar aromatic system occupied the hydrophobic pocket formed by Glutamate870, Alanine869, Glycine868, Asparagine867, Phenylalanine834, Leucine799, Asparagine798, Asparagine795, Leucine787, Asparagine786, Glutamine742, Lysine739, Phenylalanine738, Glycine737 and Proline732. It formed one H-bond with the key amino acid Asparagine795 in the active site. It also stacked between the diphosphate Cytidine (Dc1, Dc3, Dc4, Dc8 and Dc19) and diphosphate Guanosine (Dg5, Dg10 and Dg13). The cyclohexyl arm was oriented into minor groove of DNA and stabilized by formation of six H-bonds (two H-bonds with Arginine945, one H-bond with Tyrosine908, one H-bond with Leucine799, one H-bond with Glutamate870 and one H-bond with Glycine868). The elongated structure of the side chain of **10$_a$** is suggesting its action as minor groove binder (Fig. 7). These interactions of **10$_a$** may explain its highest anticancer activity.

The proposed binding mode of **11$_d$** exhibited affinity value of −95.97 kcal/mol and five H-bonds. The planar aromatic system occupied the hydrophobic pocket formed by Glutamate870, Alanine869, Glycine868, Asparagine867, Phenylalanine834, Leucine799, Asparagine795, Leucine787, Asparagine786, Glutamine742, Lysine739, Phenylalanine738, Glycine737 and Proline732. It formed one H-bond with the key amino acid Glutamine742. It also stacked between the diphosphate Cytidine (Dc3, Dc4, Dc8 and Dc19) and diphosphate Guanosine (Dg5, Dg10 and Dg13). The cyclohexyl arm was oriented into minor groove of DNA and stabilized by formation of four H-bonds (one H-bond with Arginine945, two H-bonds with Asparagine882 and one H-bond with Glycine868). The elongated structure of the side chain of **11$_d$** is suggesting its action as minor groove binder (Fig. 8). These interactions of **11$_d$** may explain its high anticancer activity.

The proposed binding mode of **8$_e$** exhibited affinity value of −88.11 kcal/mol and five H-bonds. The planar aromatic system occupied the hydrophobic pocket formed by Asparagine882, Leucine880, Glutamate870, Alanine869, Glycine868, Asparagine867, Asparagine795 and Asparagine786. It was stabilized by formation of four H-bonds with Lysine739, and one H-bond with Asparagine867. It also stacked between the diphosphate Cytidine (Dc3, Dc4 and Dc8) and diphosphate Guanosine (Dg5, Dg10 and Dg13). The small structure of compound **8e** is suggesting its intercalation into DNA (Fig. 9).

The proposed binding mode of **8$_c$** exhibited affinity value of −87.47 kcal/mol and five H-bonds. The planar aromatic system occupied the hydrophobic pocket formed by Asparagine882, Leucine880, Glutamate870, Alanine869, Glycine868, Asparagine867, Asparagine795 and Asparagine786. It was stabilized by formation of four H-bonds with Lysine739, and one H-bond with Glutamine742. It also stacked between the diphosphate Cytidine (Dc3, Dc4 and Dc8) and diphosphate Guanosine (Dg5, Dg10 and Dg13). The small structure of compound **8c** is suggesting its intercalation into DNA (Fig. 10).

As planned, our small aromatic molecules were concluded to act through two ways firstly, through non-covalent interaction with the directly bound proteins to DNA hence inhibit topoisomerase-II enzyme. The second is through non-covalently binding to double helical structures of DNA either by intercalating binder as in compounds **10$_a$** and **11$_d$** or by minor groove binding as in compounds **8$_e$** and **8$_c$** (as shown in Figs. 1, 7–10). The hydrophobic distal moieties and the long linkers and hydrogen bond acceptors and/or donors present in the structures and/or the small side chains with short linkers increased affinity towards DNA active site and act through the two above mentioned mechanisms. On the other hand, these modifications compensated hydrogen bonding and hydrophobic interactions of the reference drug doxorubicin.

2.3. *Validation of the accuracy of docking*

As cited in literature [42] if the RMSD (root mean square deviation) of the best docked conformation is ≤2.0 Å from the bound ligand in the experimental crystal, the used scoring function is successful. Therefore, the docked results were compared to the crystal structure of the bound ligand–protein complex. The obtained success rates were highly excellent as cited in Table 1. The amsacrine ligand (m-AMSA), *N*-(4-(acridin-

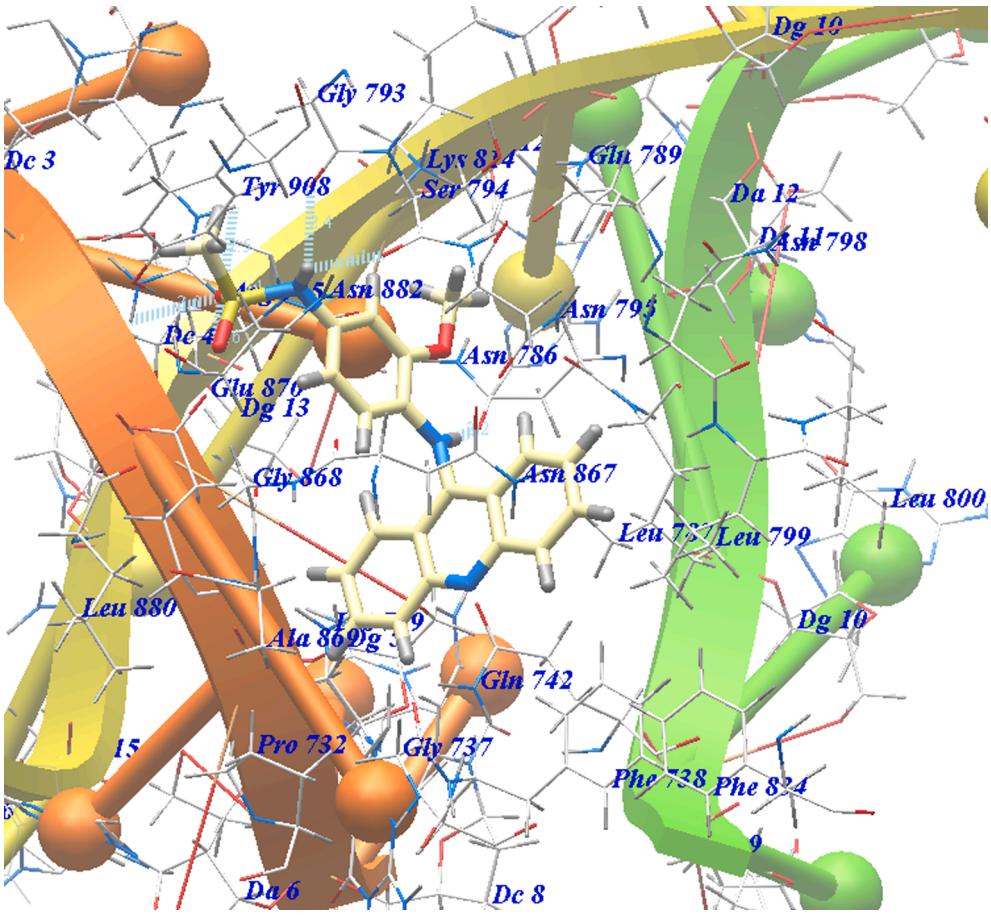

Fig. 5. Binding of amsacrine with DNA-Topo II, the hydrogen bonds are represented in blue dashed lines. (For interpretation of the references to colour in this figure legend, the reader is referred to the web version of this article.)

9-ylamino)-3-methoxyphenyl)methanesulfonamide, was docked into DNA-Topo II receptor (pdb code: 4G0U). The RMSD of the docked ligand was 0.91 Å as it seems exactly superimposed on the native bound one (Fig. 11). These results indicated the high accuracy of the docking simulation in comparison with the biological methods.

2.4. *In vitro anti-proliferative activity*

Anti-proliferative activities of the twenty four newly synthesized [1,2,4]triazolo[4,3-*a*]quinoxaline derivatives **5-14$_{a-d}$** were examined against three human tumor cell lines namely, hepatocellular carcinoma (HepG2), colorectal carcinoma (HCT-116) and breast cancer (MCF-7) using 3-[4,5-dimethylthiazol-2-yl]-2,5-diphenyltetrazolium bromide (MTT) colorimetric assay as described by Mosmann [43–45]. Doxorubicin was included in the experiments as reference cytotoxic drug. The results were expressed as growth inhibitory concentration (IC_{50}) values and summarized in Table 2. From the obtained results, it was explicated that most of the prepared compounds displayed excellent to modest growth inhibitory activity against the tested cancer cell lines. In general, investigations of the cytotoxic activity indicated that MCF-7 and HepG2 were the most sensitive cell lines to the influence of the new derivatives respectively. In particular, compounds **10$_a$**, **11$_d$** and **8$_e$** were found to be the most potent derivatives overall the tested compounds against the three HepG2, HCT116 and MCF-7 cancer cell lines with IC_{50} = (4.55 ± 0.3, 6.18 ± 0.8 and 3.93 ± 0.6 μM), (5.61 ± 0.5, 6.49 ± 0.5 and 3.71 ± 0.3 μM) and (4.66 ± 0.3, 8.08 ± 0.8 and 5.11 ± 0.7 μM) respectively. The three derivatives exhibited higher activities than **doxorubicin**, (IC_{50} = 7.94 ± 0.6, 8.07 ± 0.8 and 6.75 ± 0.4 μM respectively), against HepG2 and MCF-7 but **8$_e$** exhibited nearly the same activity against HCT116 cancer cell lines respectively.

With respect to the HepG2 hepatocellular carcinoma cell line, compounds **8$_c$, 8$_b$, 8$_a$, 11$_b$, 11$_c$, 11$_e$, 10$_b$, 14$_c$, 14$_b$** and **13$_a$** displayed the very good anticancer activities with (IC_{50} = 4.69 ± 0.3, 6.70 ± 3.7, 7.13 ± 0.6, 11.43 ± 1.0, 12.09 ± 1.3, 15.79 ± 1.4, 16.11 ± 1.5, 18.35 ± 1.7, 19.56 ± 1.8 and 21.27 ± 1.9 respectively). Compounds **8$_d$, 11$_a$, 5, 14$_d$** and **14$_a$**, with IC_{50} = 29.39 ± 2.6, 34.87 ± 3.1, 40.69 ± 3.6, 48.17 ± 3.2 and 49.41 ± 3.7 μM respectively, displayed good cytotoxicity. Compounds **12$_c$, 6, 9 and 13$_b$** with (IC_{50} ranging from 56.81 ± 3.9to 68.13 ± 4.3 μM) exhibited moderate cytotoxicity. While, compounds **12$_a$** and **12$_b$** with IC_{50} = 77.26 ± 4.6 and > 100 μM respectively, displayed the lowest cytotoxicity.

Cytotoxicity evaluation against colorectal carcinoma (HCT-116) cell line, discovered that compounds **8$_a$, 8$_b$, 8$_c$, 10$_b$, 11$_b$, 11$_c$, 11$_e$, 13$_a$, 14$_b$** and **14$_c$** displayed the very good anticancer activities with (IC_{50} ranging from 8.57 ± 0.7 to 23.97 ± 1.8 μM). Compounds **5, 6, 8$_d$, 9, 11$_a$, 12$_c$, 14$_a$** and **14$_d$**, with IC_{50} ranging from 29.60 ± 2.5 to 48.16 ± 3.8 μM respectively, displayed good cytotoxicity. Compound **13$_b$** with (IC_{50} = 50.68 ± 3.9 μM) exhibited moderate cytotoxicity. While, compounds **12$_a$** and **12$_b$** with IC_{50} = 80.56 ± 5.0 and > 100 μM respectively, displayed the lowest cytotoxicity.

Cytotoxicity evaluation against MCF-7 cell line, revealed that compounds **8$_{a-d}$, 10$_b$, 11$_b$, 11$_c$, 11$_e$, 13$_a$, 14$_b$** and **14$_c$** displayed the very good anticancer activities with (IC_{50} ranging from 4.13 ± 0.4 to 22.49 ± 1.8 μM). Compounds **5, 6, 9, 11$_a$, 12$_c$, 13$_b$, 14$_a$** and **14$_d$**, with IC_{50} ranging from 27.50 ± 2.1 to 46.37 ± 3.5 μM respectively, displayed good cytotoxicity. Compound **12$_a$** with (IC_{50} = 67.25 ± 4.7 μM) exhibited moderate cytotoxicity. While, compound **12$_b$** with IC_{50} = 81.46 ± 5.2 μM, displayed the lowest cytotoxicity.

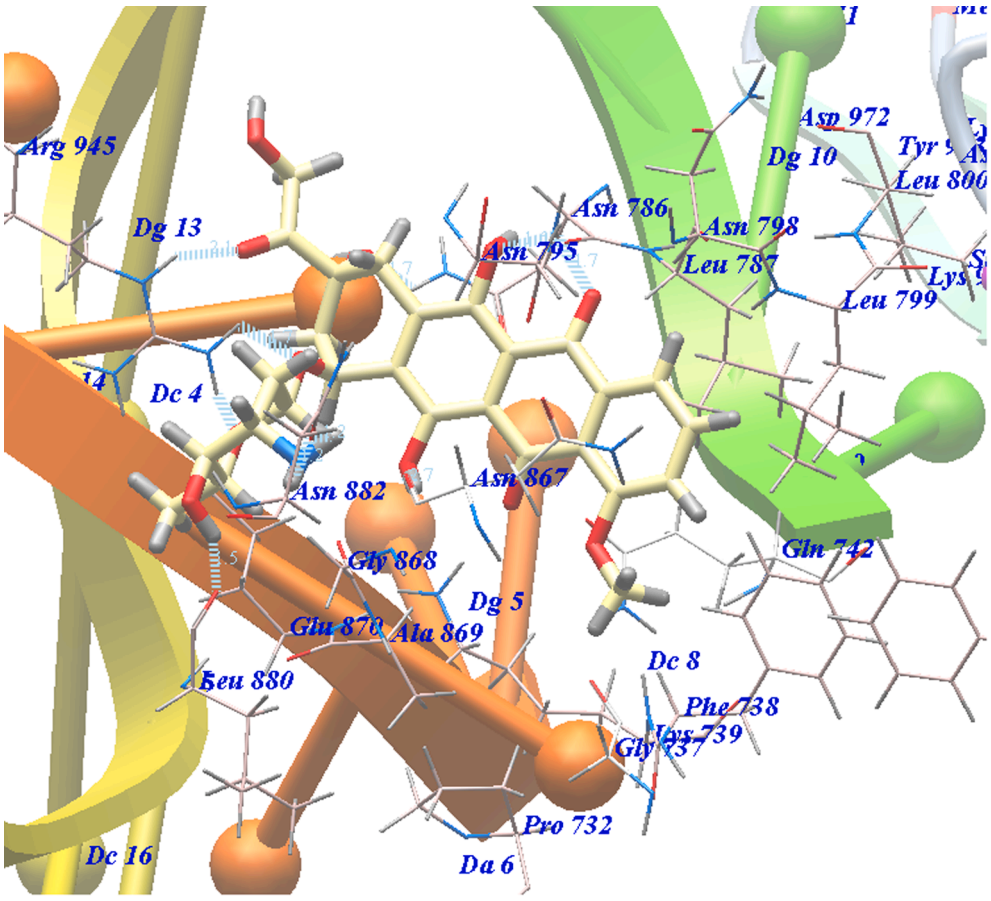

Fig. 6. Binding of doxorubicin with DNA-Topo II, the hydrogen bonds are represented in blue dashed lines. (For interpretation of the references to colour in this figure legend, the reader is referred to the web version of this article.)

2.5. In vitro DNA/methyl green assay

The most active anti-proliferative derivatives **$8_{a\text{-}e}$, $10_{a,b}$, $11_{b\text{-}e}$, 13_a** and **$14_{b,c}$** were further evaluated for their DNA-binding affinity which revealed the ability of these compounds to intercalate DNA. It was carried out by use of methyl green dye according to the reported procedure described by Burre *et al* [20,21,46]. The results of DNA-binding affinity were obtained as IC_{50} values and summarized in Table 3. Doxorubicin, as one of the most powerful DNA intercalators, was used as a positive control.

The tested compounds displayed very good to moderate DNA-binding affinities. Compounds **10_a 11_d, 8_e, 8_c, 8_a** and **8_b** displayed the highest binding affinities. These compounds potently intercalate DNA at decreased IC_{50} values of 25.27 ± 1.2, 27.47 ± 2.1, 27.54 ± 3.2, 27.78 ± 1.3, 29.15 ± 1.8 and 30.23 ± 3.7 μM respectively, which were less than that of doxorubicin (31.27 ± 1.8). Compounds **10_b, 11b, 11c, 11e, 14_b** and **14_c** exhibited good DNA-binding affinities with IC_{50} values ranging from 35.33 ± 1.8 to 48.13 ± 2.5 μM. Finally, compounds **13_a** and **8_d** showed moderate DNA-binding affinities with IC_{50} values of 50.56 ± 2.7 and 63.26 ± 3.2 μM respectively.

2.6. In vitro Topoisomerase II inhibitory activity

The most active cytotoxic compounds **8_a, 8_b, 8_c, 8_e, 10_a** and **11_d** were selected to evaluate their inhibitory activities against Topo II enzyme. Topo II catalytic activity was tested according to the reported procedure [20]. For comparison, one representative drug, doxorubicin, was also tested using the same procedure as a positive control. The results were recorded as a 50% inhibition- concentration values (IC_{50}) calculated from the concentration-inhibition response curve and summarized in Table 4.

As shown in Table 4, all the tested compounds could interfere with the Topo II activity. They exhibited very good inhibitory activities with IC_{50} values ranging from 0.379 ± 0.07 to 0.813 ± 0.14 μM that were lower than that of doxorubicin (IC_{50} = 0.94 ± 0.4 μM). For a great extent, the reported results were in agreement with that of *in vitro* cytotoxicity activity, DNA binding and molecular modeling studies. Among them, compounds **10_a** and **8_e** were found to be the most potent derivatives at very low IC_{50} value of 0.379 ± 0.07 and 0.384 ± 0.17 μM respectively. Also, compounds **11_d** and **8_c** possessed low IC_{50} values of 0.417 ± 0.07 and 0.521 ± 0.05 μM, respectively), while compounds **8_a** and **8_b** (IC_{50} = 0.715 ± 0.06 and 0.813 ± 0.14 μM, respectively).

2.7. Correlation study

To confirm the obtained biological data, that states the tested compounds possess a cytotoxic effect in the tested cell lines through interaction with DNA inhibiting the Top-II enzymes, we perform further significant statistic study to imply the correlation between DNA-Top-II inhibiting activity and the induced cytotoxicity. The DNA binding activity of the studied compounds were plotted against their corresponding cytotoxicity in simple linear regression relationship for each cell line, the obtained coefficients of R squares and P–values approves a very strong correlation between the DNA binding activity and cytotoxicity of tested compounds (for HepG-2 R^2 = 0.9866, p-value = 0.0001, for HCT-116 R^2 = 0.9886, p-value = 0.0001, for MCF-7 R^2 = 0.9780, p-value = 0.0001). In addition, there is a significant connection of DNA binding activity of the established compounds with their equivalent Top-II inhibitory activity (R^2 = 0.7938, p-value = 0.0172) (Fig. 12).

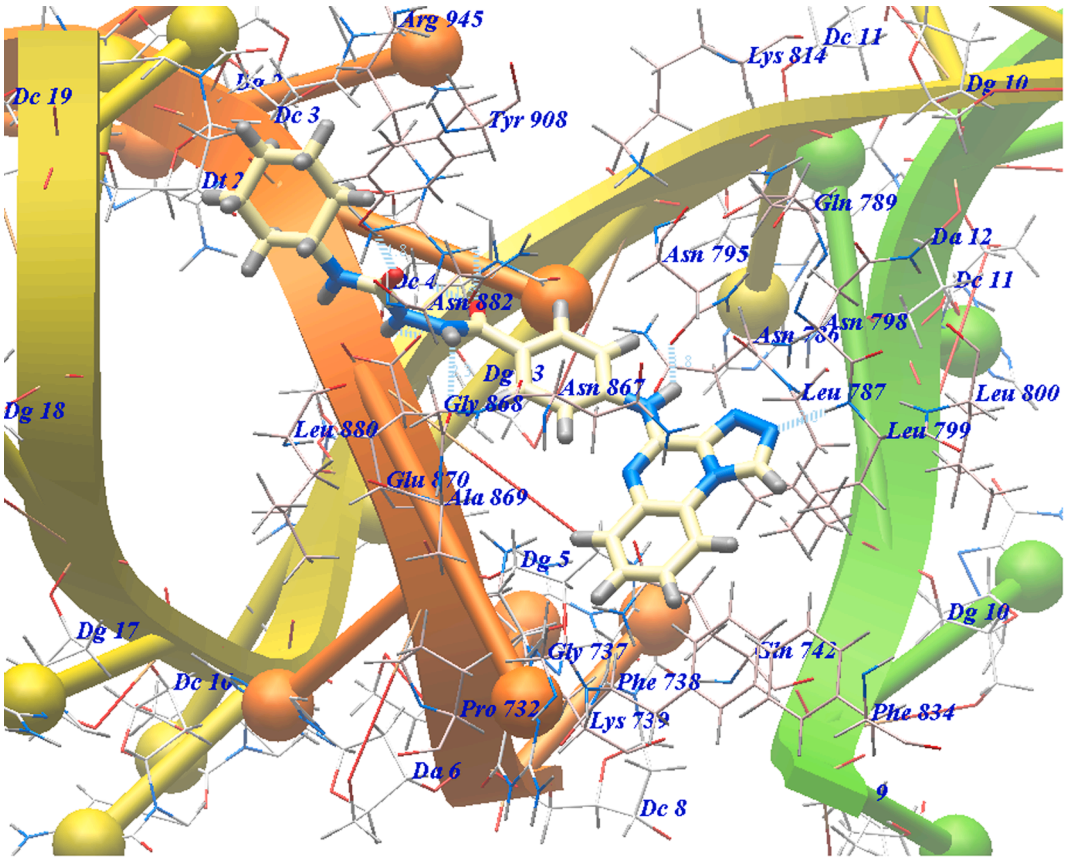

Fig. 7. Predicted binding mode for $\mathbf{10_a}$ with DNA.

2.8. Structure activity relationship (SAR)

The preliminary SAR study has focused on the effect of hydrophobic and electronic nature of the substituents used in this study. Also, it focused on the effect of the length of linkers used which attached to the distal moieties. The data obtained revealed that, the tested compounds displayed different levels of anticancer activity and possessed a distinctive pattern of selectivity against the MCF-7 and HepG2 cell lines respectively. The [1,2,4]triazolo[4,3-*a*]quinoxaline scaffold, amines, ester, acid hydrazide, semicarbazide, thiosemicarbazide, sulfonamides, sulfonylurea and/or sulfonythiourea linkers containing (HBA-HBD), lipophilicity and electronic nature exhibited an important role in DNA intercalations and consequently anticancer activity. Generally, hydrophobic electron donating groups displayed higher activities than the hydrophilic and/or electron withdrawing ones respectively. The presence of the hydrophobic electron donating cyclohexyl distal moieties linked to the chromophore through semicarbazide, thiosemicarbazide and/or NH linkers as in compounds $\mathbf{10_a}$, $\mathbf{11_d}$ and $\mathbf{8_c}$ respectively was found to be responsible for their higher anticancer activities. Also the presence of the hydrophobic electron donating diethyl attached through NH linker exhibited higher activities. The presence of long linker as in compounds $\mathbf{10_a}$, $\mathbf{11_d}$ enables the distal moieties to form different hydrophobic and hydrogen bonding interactions and these long arms oriented into the minor groove suggesting their action as minor groove binders. On the other hand, the NH short linker enables the scaffold and the distal moieties to be sandwiched between the base pairs of DNA suggesting their action as DNA intercalators. Moreover, the non-covalent bonding with the amino acids adjacent to DNA in the active site suggesting that our derivatives act through topoisomerase II enzyme inhibition also.

From the structure of the synthesized derivatives and the data shown in Table 2 we can divide these tested compounds into four groups. The first group is compounds **5, 6,** $\mathbf{8_{a\text{-}e}}$ and **9**. In this group short chain NH linkers were used. In this group the hydrophobic electron donating (+inductive [+I]) aliphatic groups such as diethyl, cyclohexyl, butyl and/or propyl in compounds $\mathbf{8_e}$, $\mathbf{8_c}$, $\mathbf{8_b}$ and $\mathbf{8_a}$ showed higher anticancer activities than the hydrophilic electron withdrawing (- mesomeric [−M], [−I]) carboxylic, hydrophobic electron withdrawing (−M, −I) ester and/or hydrophilic electron withdrawing (−M, −I) acid gydrazide in compounds **5, 6** and **9** respectively. The unsubstituted benzyl moiety $\mathbf{8_d}$ exhibited higher activities than the 4-substituted phenyl containing derivatives **5, 6** and **9** respectively. With respect to HepG2 the hydrophobic electron donating (+I) diethyl moiety $\mathbf{8e}$ exhibited higher activity than cyclohexyl $\mathbf{8_c}$, butyl $\mathbf{8_b}$, propy $\mathbf{8_a}$, the hydrophobic electron withdrawing benzyl $\mathbf{8_d}$, hydrophilic electron withdrawing (−M, −I) acid **5**, hydrophobic (−M, −I) ester **6**, hydrophilic (−M, −I) hydrazide **9** respectively. With respect to HCT116 the hydrophobic electron donating (+I) displayed higher activities than hydrophilic and/or hydrophobic electron withdrawing (−M, −I) moieties and the order of activity is $\mathbf{8_e > 8_a > 8_c > 8_b > 8_d > 9 > 5 > 6}$. On the other hand, regarding MCF-7 the order of activity is $\mathbf{8_c > 8_b > 8_a > 8_e > 8_d > 9 > 5 > 6}$.

The second group is semicarbazides $\mathbf{10_{a,b}}$ and thiosemicarbazides $\mathbf{11_{a\text{-}e}}$ in this group the terminal distal moieties and long linkers designed played an important role in activity. Generally, the cyclohexyl distal moiety attached to semicarbazide linker e.g. $\mathbf{10_a}$ showed higher activities than that attached to thiosemicarbazide linker $\mathbf{11_d}$ against both HepG2 and HCT116 cancer cell lines while $\mathbf{11_d}$ exhibited higher activity than $\mathbf{10_a}$ against MCF-7 cell lines. On the other hand, the hydrophobic electron withdrawing phenyl group attached to thiosemicarbazide linker $\mathbf{11_e}$ displayed higher activities than that attached to semicarbazide one $\mathbf{10_b}$ against the three MCF-7, HepG2 and HCT116 cancer cell lines respectively. The hydrophobic electron donating (+I) cyclohexyl group $\mathbf{10_a}$ displayed higher activities than butyl $\mathbf{11_c}$, propyl $\mathbf{11_b}$,

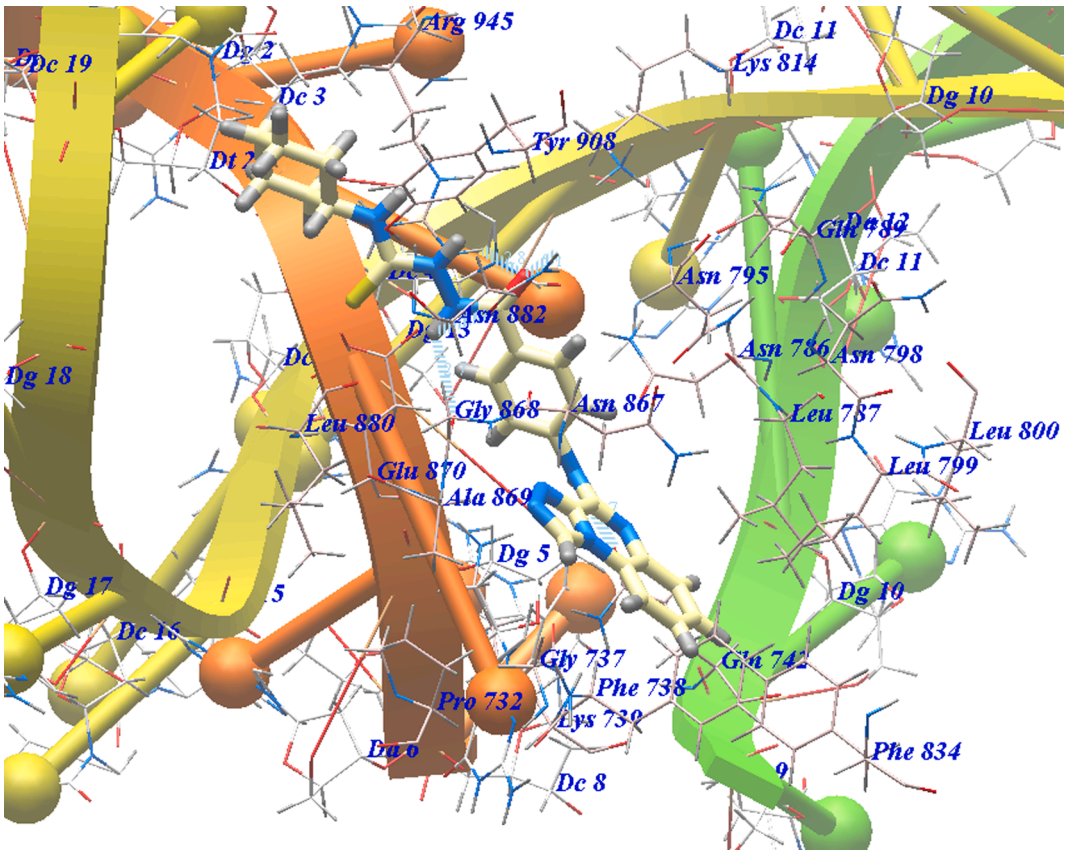

Fig. 8. Predicted binding mode for $\mathbf{11_d}$ with DNA-Topo II.

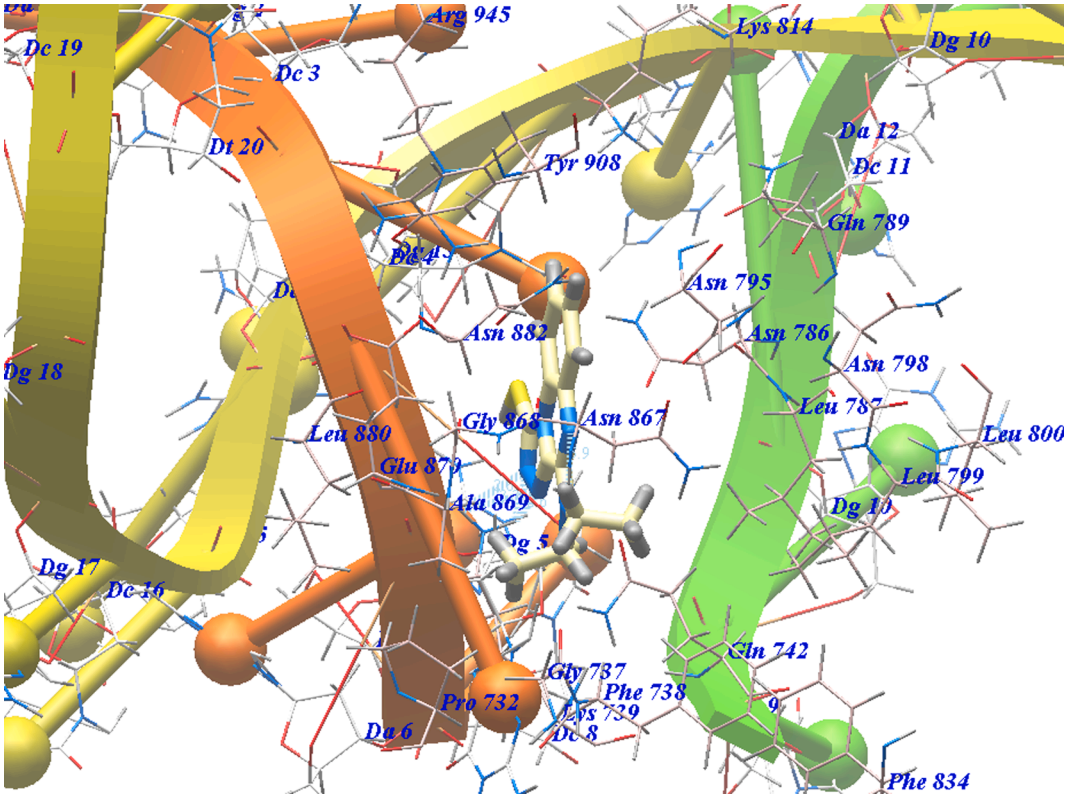

Fig. 9. Predicted binding mode for $\mathbf{8_e}$ with DNA-Topo II.

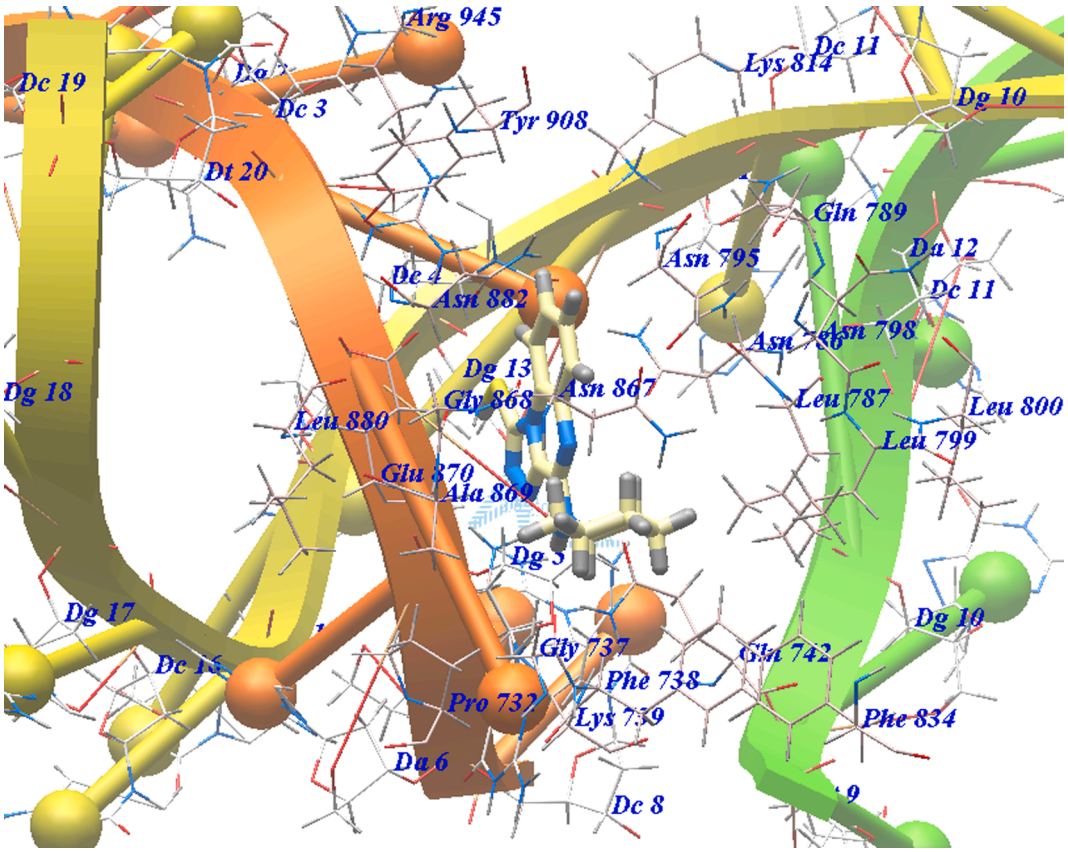

Fig. 10. Predicted binding mode for $\mathbf{8_c}$ with DNA-Topo II.

phenyl $\mathbf{11_e}$ and/or ethyl $\mathbf{11_a}$ against the three MCF-7, HepG2 and HCT116 cancer cell lines respectively except the propyl derivative $\mathbf{11_b}$ which exhibited higher activity than the butyl one $\mathbf{11_c}$ against MCF-7 cancer cell lines.

In the third group $\mathbf{12_{a\text{-}c}}$, the substituted sulfonamides with six membered pyrimidine moiety $\mathbf{12_c}$ showed higher activities than the unsubstituted $\mathbf{12_a}$ and the five membered thiazole $\mathbf{12_b}$ respectively against the three cancer cell lines.

The fourth group is sulfonylurea $\mathbf{13_{a,b}}$ and thiosulfonylurea $\mathbf{14_{a\text{-}e}}$ derivatives. In this group generally, the terminal distal phenyl group attached to thiosulfonylurea linker $\mathbf{14_d}$ showed higher activities than the aliphatic ethyl one $\mathbf{14_a}$ and the phenyl $\mathbf{13_a}$ that attached to sulfonylurea linker respectively against the three cancer cell lines. The cyclohexyl (+I) moiety $\mathbf{13_a}$ exhibited higher activity than that substituted with phenyl one $\mathbf{13_b}$ against the three cancer cell lines. On the other hand, the hydrophobic electron donating aliphatic butyl group $\mathbf{14_c}$ displayed higher activities than propyl $\mathbf{14_b}$ and cyclohexyl $\mathbf{13_a}$ and the aromatic phenyl ones $\mathbf{14_d}$ and $\mathbf{13_b}$ respectively against the three cancer cell lines except the propyl derivative $\mathbf{14_b}$ which exhibited higher activities than the butyl one $\mathbf{14_c}$ against both HepG2 and HCT116 cancer cell lines.

The data obtained from DNA binding in Table 3 we can concluded that, the presence of the hydrophobic distal cyclohexyl moiety connected to the semicarbazide linker $\mathbf{10_a}$ exhibited higher DNA binding activity than that attached to thiosemicarbazide $\mathbf{11_d}$ and/or NH ones $\mathbf{8_c}$ respectively. The diethyl amine derivative $\mathbf{8_e}$ displayed higher activity than cyclohexyl amine $\mathbf{8_c}$, propyl amine $\mathbf{8_a}$, butyl $\mathbf{8_b}$ and benzyl amines $\mathbf{8_d}$ respectively. Moreover, the hydrophobic electron donating butyl group attached to thiosemicarbazide linker $\mathbf{11_c}$ showed higher DNA binding activity than the propyl $\mathbf{11_b}$, phenyl $\mathbf{11_e}$ and the phenyl one attached to semicarbazide linker $\mathbf{10_b}$. Finally, propyl group linked to sulfonylthiourea linker $\mathbf{14_b}$ displayed higher DNA binding than the butyl $\mathbf{14_c}$ and the cyclohexyl group that attached to sulfonylurea linker $\mathbf{13_a}$ respectively.

The data obtained from Topo II enzyme inhibition assay in Table 4 it was found that, the presence of the hydrophobic distal cyclohexyl moiety joined to the semicarbazide linker $\mathbf{10_a}$ exhibited higher Topo II inhibitory activity than the diethyl attached to NH linker $\mathbf{8_e}$, the cyclohexyl attached to thiosemicarbazide $\mathbf{11_d}$ and/or NH ones $\mathbf{8_c}$ respectively. Moreover, diethyl amine $\mathbf{8_e}$ displayed higher activity than cyclohexyl amine $\mathbf{8_c}$, propyl amine $\mathbf{8_a}$ and butyl amine $\mathbf{8_b}$ respectively.

3. Conclusion

In summary, twenty four new [1,2,4]triazolo[4,3-*a*]quinoxaline based derivatives have been designed, synthesized and evaluated for their anticancer activities against three human tumor cell lines hepatocellular carcinoma (HepG2), colorectal carcinoma (HCT-116) and breast cancer (MCF-7) as DNA intercalators and Top II enzyme inhibitors. All the tested compounds showed variable anticancer activities. The molecular design was performed to investigate the binding mode of the proposed compounds with DNA-Topo II active site. The data obtained from biological testing highly correlated with that obtained from molecular modeling studies. In general, investigations of the cytotoxic activity indicated that MCF-7 and HepG2 were the most sensitive cell lines to the influence of the new derivatives respectively. In particular, compounds $\mathbf{10_a}$, $\mathbf{11_d}$ and $\mathbf{8_e}$ were found to be the most potent derivatives overall the tested compounds against the three HepG2, HCT116 and MCF-7 cancer cell lines with IC_{50} = (4.55 ± 0.3, 6.18 ± 0.8 and 3.93 ± 0.6 μM), (5.61 ± 0.5, 6.49 ± 0.5and 3.71 ± 0.3 μM) and (4.66 ± 0.3, 8.08 ± 0.8 and 5.11 ± 0.7 μM) respectively. The three derivatives exhibited higher activities than **doxorubicin**, (IC_{50} = 7.94 ± 0.6, 8.07 ± 0.8 and 6.75 ± 0.4 μM respectively), against HepG2 and MCF-7 but $\mathbf{8_e}$ exhibited nearly the same activity against HCT116 cancer cell lines

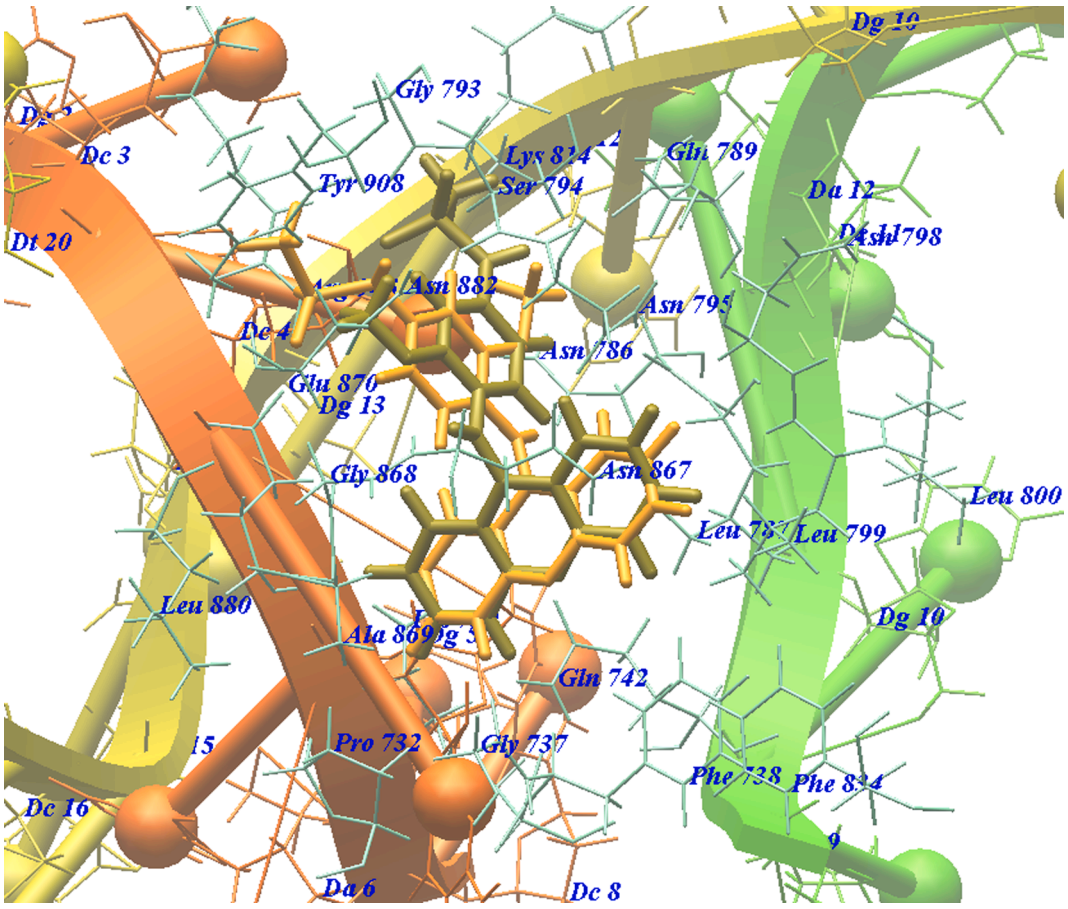

Fig. 11. Superimposition of the co-crystallized ligand amsacrine on the native bound one with DNA-Topo II.

Table 2
In vitro cytotoxic activities of the newly synthesized compounds against HepG2, HCT-116 and MCF-7cell lines.

Compound	IC_{50} (μM)[a]		
	HepG2	HCT116	MCF-7
5	40.69 ± 3.6	36.47 ± 3.3	32.91 ± 2.4
6	59.23 ± 3.9	47.30 ± 3.9	41.56 ± 3.0
8_a	7.13 ± 0.6	8.57 ± 0.7	4.96 ± 0.3
8_b	6.70 ± 3.7	9.90 ± 3.6	4.57 ± 2.7
8_c	4.69 ± 0.3	9.10 ± 0.8	4.13 ± 0.4
8_d	29.39 ± 2.6	29.60 ± 2.5	22.49 ± 1.8
8_e	4.66 ± 0.3	8.08 ± 0.8	5.11 ± 0.7
9	61.37 ± 4.0	36.04 ± 3.1	27.50 ± 2.1
10_a	4.55 ± 0.3	6.18 ± 0.8	3.93 ± 0.6
10_b	16.11 ± 1.5	18.61 ± 1.6	10.89 ± 1.0
11_a	34.87 ± 3.1	35.86 ± 2.9	29.12 ± 2.3
11_b	11.43 ± 1.0	14.16 ± 1.3	9.38 ± 0.8
11_c	12.09 ± 1.3	13.29 ± 1.2	7.48 ± 0.8
11_d	5.61 ± 0.5	6.49 ± 0.5	3.71 ± 0.3
11_e	15.79 ± 1.4	17.38 ± 1.5	10.25 ± 0.9
12_a	77.26 ± 4.6	80.56 ± 5.0	67.25 ± 4.7
12_b	>100	>100	81.46 ± 5.2
12_c	56.81 ± 3.9	48.16 ± 3.8	44.24 ± 3.3
13_a	21.27 ± 1.9	23.97 ± 1.8	15.24 ± 1.4
13_b	68.13 ± 4.3	50.68 ± 3.9	46.37 ± 3.5
14_a	49.41 ± 3.7	41.27 ± 3.5	37.82 ± 2.6
14_b	19.56 ± 1.8	20.35 ± 1.7	12.76 ± 1.1
14_c	18.35 ± 1.7	21.81 ± 1.8	13.80 ± 1.2
14_d	48.17 ± 3.2	39.44 ± 3.2	35.68 ± 3.1
Doxorubicin	7.94 ± 0.6	8.07 ± 0.8	6.75 ± 0.4

[a] IC_{50} values are the mean ± S.D. of three separate experiments.

Table 3
DNA binding affinity of some tested compounds.

Compound	DNA binding IC_{50} (μM)	Compound	DNA binding IC_{50} (μM)
8_a	29.15 ± 1.8	**11_c**	35.33 ± 1.8
8_b	30.23 ± 3.7	**11_d**	27.47 ± 2.1
8_c	27.78 ± 1.3	**11_e**	42.65 ± 3.5
8_d	63.26 ± 3.2	**13_a**	50.56 ± 2.7
8_e	27.54 ± 3.2	**14_b**	45.89 ± 2.5
10_a	25.27 ± 1.2	**14_c**	48.13 ± 2.5
10_b	45.09 ± 1.2	**Doxorubicin**	31.27 ± 1.8
11_b	37.23 ± 4.2		

Table 4
Topoisomerase II inhibitory activity of the most potent compounds.

Compound	Top-II assay IC_{50} (μM)[a]	Compound	Top-II assay IC_{50} (μM)[a]
8_a	0.715 ± 0.06	**10_a**	0.379 ± 0.07
8_b	0.813 ± 0.14	**11_d**	0.417 ± 0.07
8_c	0.521 ± 0.05	**Doxorubicin**	0.940 ± 0.40
8_e	0.384 ± 0.17		

respectively. The most active derivatives **$8_{a\text{-}e}$, $10_{a,b}$, $11_{b\text{-}e}$, 13_a** and **$14_{b,c}$** were evaluated for their DNA binding activities. The tested compounds displayed very good to moderate DNA-binding affinities. Compounds **10_a 11_d, 8_e, 8_c, 8_a** and **8_b** displayed the highest binding affinities. These compounds potently intercalate DNA at decreased IC_{50} values of 25.27 ± 1.2, 27.47 ± 2.1, 27.54 ± 3.2, 27.78 ± 1.3, 29.15 ± 1.8 and 30.23 ± 3.7 μM respectively, which were less than that of doxorubicin (31.27 ± 1.8). Furthermore, the most active cytotoxic compounds **8_a, 8_b, 8_c, 8_e, 10_a** and **11_d** were selected to evaluate their inhibitory activities against

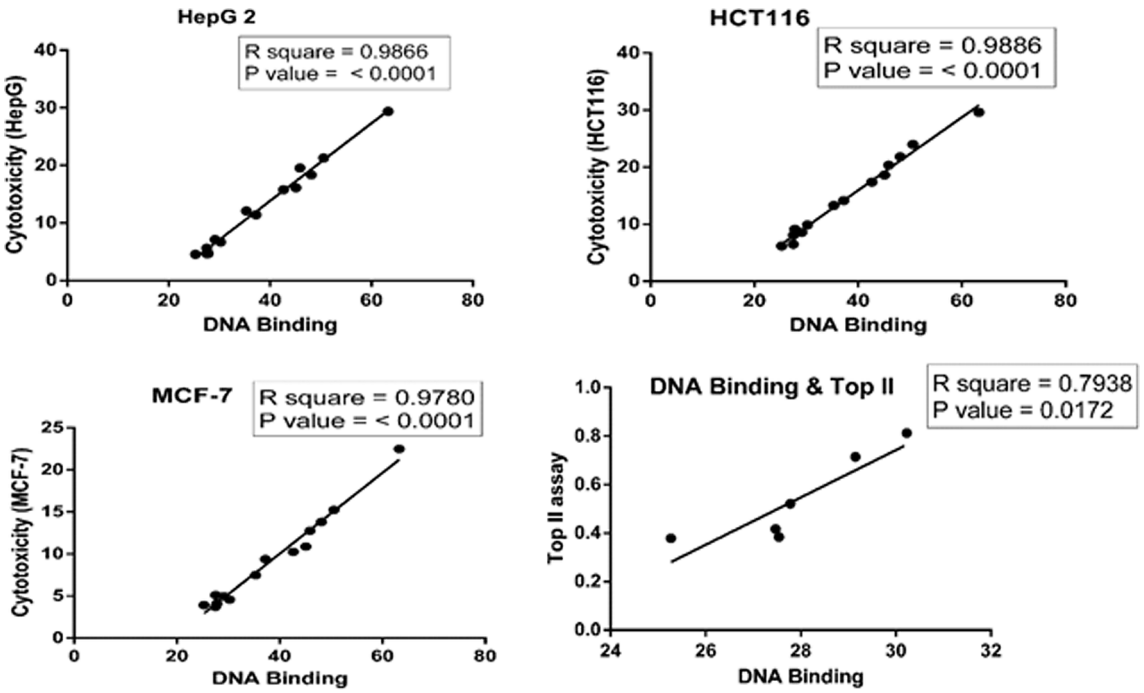

Fig. 12. Correlation between DNA binding, cytotoxicity and Top-II inhibition.

Topo II enzyme. All the tested compounds could interfere with the Topo II activity. They exhibited very good inhibitory activities with IC_{50} values ranging from 0.379 ± 0.07 to 0.813 ± 0.14 μM that were lower than that of doxorubicin (IC_{50} = 0.94 ± 0.4 μM). For a great extent, the reported results were in agreement with that of *in vitro* cytotoxicity activity, DNA binding and molecular modeling studies.

4. Experimental

4.1. Chemistry

4.1.1. General

All melting points were carried out by open capillary method on a Gallen kamp Melting point apparatus at faculty of pharmacy Al-Azhar University and were uncorrected. The infrared spectra were recorded on pye Unicam SP 1000 IR spectrophotometer at Pharmaceutical analytical Unit, Faculty of Pharmacy, Al-Azhar University using potassium bromide disc technique. Proton magnetic resonance ^{1}HNMR spectra were recorded on a Bruker 400 Megahertz-nuclear magnetic resonance (400 MHZ-NMR) spectrophotometer at Microanalytical Unit, Faculty of pharmacy, Ain Shams University and on GEMINI-400BB "NMR spectrometer at Chemical Laboratories of Ministry of Defense, Cairo. Carbon-13 (C13) nuclear magnetic resonance (^{13}CNMR) spectra were recorded on a Bruker 100 Megahertz-nuclear magnetic resonance (100 MHZ-NMR) spectrophotometer at Microanalytical Unit, Faculty of pharmacy, Cairo University. Tetramethylsilane (TMS) was used as internal standard and chemical shifts were measured in δ scale one part per million (ppm). The mass spectra were carried out on Direct Probe Controller Inlet part to Single Quadropole mass analyzer in Thermo Scientific Gas chromatography–mass spectrometry (GCMS) model ISQ LT using Thermo X-Calibur software at the Mycology and Biotechnology Regional Center, Al-Azhar University. Elemental analyses (C, H, N) were performed on a carbon hydrogen and nitrogen (CHN) analyzer at Mycology and Biotechnology Regional Center, Al-Azhar University. All compounds were within ±0.4 of the theoretical values. The reactions were monitored by thin-layer chromatography (TLC) using TLC sheets precoated with UV fluorescent silica gel Merck 60 F254 plates and were visualized using ultraviolet (UV) lamp and different solvents as mobile phases.

Compounds, 2,3-(1*H*,4*H*)-quinoxalinedione **1,** 2,3-dichloroquinoxaline **2,** 2-chloro-3-hydrazinylquinoxaline **3,** 4-chloro[1,2,4]triazolo [4,3-*a*]quinoxaline **4** and 4-chloro-[1,2,4]triazolo[4,3-*a*]quinoxaline-1-thiol **(7)** were obtained according to the reported procedures [21,39,40].

4.1.2. General procedure for synthesis of target compounds (5) and (6)

Equimolar quantities of 4-Chloro-[1,2,4]triazolo[4,3-*a*]quinoxaline **4** (0.01 mol) and the appropriate 4-aminobenzoate derivative (0.01 mol) namely; methyl 4-aminobenzoate and/or 4-aminobenzoic acid in acetonitrile (CH_3CN) (20 ml) in the presence of few drops of triethylamine (TEA) were heated under reflux for 5 h. The formed precipitate was filtered, washed with *n*-hexane, and air dried to get the corresponding target compounds **5** and **6** respectively.

4.1.2.1. Methyl 4-([1,2,4]triazolo[4,3-a]quinoxalin-4-ylamino)benzoate (5). Yield, 90%; m.p. 170–2 °C; $IR_{\nu max}$ (cm^{-1}): 3243 (NH), 3090 (C—H aromatic), 2965 (C—H aliphatic), 1725 (CO ester); ^{1}HNMR (400 MHz, DMSO-d_6): 3.47 (s, 3H, CH_3), 7.42 (dd, *J* = 8, 8.8 Hz, H, H-7 quinox.), 7.48 (dd, *J* = 8.4, 8.8 Hz, 1H, H-8 quinox.), 7.71 (d, *J* = 8 Hz, 1H, H-9 quinox.), 7.89 (dd, *J* = 8.4, 10 Hz, 2H, H-3 and H-5 phenyl.), 8.18 (d, *J* = 8 Hz, 1H, H-6 quinox.), 8.32 (dd, *J* = 8.4, 10 Hz, 2H, H-2 and H-6 phenyl), 10.01 (s, 1H, CH triazole), 10.53 (s, 1H, **NH**-ph) (D_2O exchangeable); Anal. Calcd. for $C_{17}H_{13}N_5O_2$ (319.32): C, 63.94; H, 4.10; N, 21.93. Found: C, 64.08; H, 4.23; N, 21.88.

4.1.2.2. 4-([1,2,4]Triazolo[4,3-a]quinoxalin-4-ylamino)benzoic acid (6). Yield, 90%; m.p. 310–2 °C; $IR_{\nu max}$ (cm^{-1}): 3247 (NH, OH), 3080 (C—H aromatic), 1710 (C═O carboxylic); ^{1}H NMR (400 MHz, DMSO-d_6): 7.49 (dd, 1H, *J* = 8.4, 8 Hz, H-7ofquinoxaline),7.56 (dd, *J* = 8.4, 8 Hz, 1H, H-8 of quinox.), 7.80 (d, 1H, *J* = 8 Hz, H-9 of quinox.), 7.96 (dd, *J* = 8.8, 10 Hz, 2H, H-3 and H-5of phenyl), 8.25 (d, *J* = 8 Hz, 1H, H-6 of quinox.), 8.35 (dd, *J* = 8.8, 10 Hz, 2H, H-2 and H-6 of phenyl), 10.06 (s, 1H, CH of triazole), 10.58 (s, 1H, **NH**-ph) (D_2O exchangeable), 12.66 (s, 1H, OH) (D_2O exchangeable); MS (*m/z*): 305 (M^+, 91.43%), 304 (base beak, 100%), 276 (17.76%), 76 (20.69%); Anal. Calcd. for $C_{16}H_{11}N_5O_2$ (305.30): C, 62.95; H, 3.63; N, 22.94.

Found: C, 63.12; H, 3.80; N, 22.89.

*4.1.3. General procedure for synthesis of target compounds (**8**$_{a-e}$)*

A mixture of compound **4** (0.5 g, 0.002 mol) and the appropriate amine namely propyl amine, butyl amine, cyclohexyl amine, benzyl amine and/or diethyl amine (0.003 mol) in dry MeCN (10 ml) in the presence of drops of TEA was heated under reflux for 6 h. then concentrated. The precipitated solid were filtered and crystallized from ethanol to afford the desired products **8**$_{a-e}$ respectively.

*4.1.3.1. 4-(Propylamino)-[1,2,4]triazolo[4,3-a]quinoxaline-1-thiol (**8**$_a$).* Yield, 90%; m.p. 260–2 °C; IR$_{\nu max}$ (cm^{-1}): 3294 (NH), 3063 (C—H aromatic), 2950 (C—H aliphatic), 2569 (SH); ^{1}HNMR (400 MHz, DMSO-d_6): 0.95 (t, J = 7.6 Hz, 3H, CH_3), 1.65–1.72 (m, J = 7.6 Hz, 2H, CH_2-**CH_2**-CH_3), 3.48 (t, J = 7.6 Hz, 2H, **CH_2**-CH_2-CH3), 6.95 (dd, J = 7.2 Hz, 1H, H-7 quinox.), 7.02 (dd, J = 7.6, 8 Hz, 1H, H-8 quinox.), 7.21 (d, J = 8 Hz, 1H, H-9 quinox.), 7.23–7.25 (d, 1H, H-6 quinox.), 7.65–7.67 (s, 1H, NH) (D_2O exchangeable), 10.65 (s, 1H, SH) (D_2O exchangeable); MS (*m/z*): 259 (M$^+$, 19.90%), 236 (58.92%), 202 (83.23%), 173 (83.90%), and 59 (base beak, 100%); Anal. Calcd. for $C_{12}H_{13}N_5S$ (259.33): C, 55.58; H, 5.05; N, 27.01. Found: C, 55.79; H, 5.32; N, 27.35.

*4.1.3.2. 4-(Butylamino)-[1,2,4]triazolo[4,3-a]quinoxaline-1-thiol (**8**$_b$).* Yield, 95%; m.p. 262–4 °C; IR$_{\nu max}$ (cm^{-1}): 3375 (NH), 3013 (C—H aromatic), 2968 (C—H aliphatic), 2562 (SH); ^{1}HNMR (400 MHz, DMSO-d_6): 1.00 (t, J = 7.6 Hz, 3H, CH_3), 1.20–1.40 (m, 2H, CH_2-CH_2-**CH_2**-CH_3), 1.55–1.68 (m, 2H, CH_2-**CH_2**-CH_2-CH_3), 3.52 (t, J = 7.6 Hz, 2H, **CH_2**-CH_2-CH_2-CH_3), 6.99 (dd, J = 7.2, 8 Hz, 1H, H-7 quinox.), 7.04 (dd, J = 7.6, 8 Hz, 1H, H-8 quinox.), 7.24 (d, J = 7.2 Hz, 1H, H-9 quinox.), 7.67 (d, J = 7.2 Hz, 1H, H-6 quinox.), 7.68 (s, 1H, NH) (D_2O exchangeable), 10.70 (s, 1H, SH) (D_2O exchangeable); Anal. Calcd. for $C_{13}H_{15}N_5S$ (273.36): C, 57.12; H, 5.53; N, 25.62. Found: C, 56.98; H, 5.62; N, 25.80.

*4.1.3.3. 4-(Cyclohexylamino)-[1,2,4]triazolo[4,3-a]quinoxaline-1-thiol (**8**$_c$).* Yield, 95%; m.p. 267–9 °C; IR$_{\nu max}$ (cm^{-1}): 3283 (NH), 3063 (C—H aromatic), 2929 (C—H aliphatic), 2559 (SH); ^{1}HNMR (400 MHz, DMSO-d_6): 1.20–1.81 (m, 10*H*, C-2, C-3, C-4, C-5, C-6 cyclohexyl), 4.02–4.07 (m, 1H, C-1 cyclohexyl) 7.00 (dd, J = 8, 8.8 Hz, 1H, H-7 quinox.), 7.03 (dd, J = 8, 8.8 Hz, 1H, H-8 quinox.), 7.21 (d, J = 8 Hz, 1H, H-9 quinox.), 7.25 (d, J = 8 Hz, 1H, H-6 quinox.), 7.28 (s, 1H, NH) (D_2O exchangeable), 10.82 (s,1H, SH) (D_2O exchangeable); Anal. Calcd. for $C_{15}H_{17}N_5S$ (299.40): C, 60.18; H, 5.72; N, 23.39. Found: C, 60.04; H, 5.87; N, 23.52.

*4.1.3.4. 4-(Benzylamino)-[1,2,4]triazolo[4,3-a]quinoxaline-1-thiol (**8**$_d$).* Yield, 90%; m.p. 271–3 °C; IR$_{\nu max}$ (cm^{-1}): 3275 (NH), 3097 (C—H aromatic), 2990 (C—H aliphatic), 2567 (SH); ^{1}HNMR (400 MHz, DMSO-d_6): 4.58 (s, 2H, CH_2), 6.97 (dd, J = 7.6, 8 Hz, 1H, H-7 quinox.), 7.06 (dd, J = 7.6, 8 Hz, 1H, H-8 quinox.), 7.21 (d, J = 7.6 Hz, 1H, H-9 quinox.), 7.25 (d, J = 8 Hz, 1H, H-6 quinox.), 7.35–7.42 (m, 5H, H-2, H-3, H-4, H-5, H-6 phenyl), 8.28 (s, 1H, NH) (D_2O exchangeable), 10.77 (s, 1H, SH) (D_2O exchangeable); Anal. Calcd. for $C_{16}H_{13}N_5S$ (307.38): C, 62.52; H, 4.26; N, 22.78. Found: C, 62.79; H, 4.38; N, 22.91.

*4.1.3.5. 4-(Diethylamino)-[1,2,4]triazolo[4,3-a]quinoxaline-1-thiol (**8**$_e$).* Yield, 95%; m.p. 290–2 °C; IR$_{\nu max}$ (cm^{-1}): 3350 (NH), 3010 (C—H aromatic), 2779 (C—H aliphatic), 2569 (SH); ^{1}HNMR (400 MHz, DMSO-d_6): 1.17–1.21 (m, 6H, 2CH_3), 2.97–3.02 (m, 4H, 2CH_2), 7.02 (dd, J = 7.6, 8.8 Hz, 1H, H-7 quinox.), 7.10 (dd, J = 7.2, 7.6 Hz, 1H, H-8 quinox.), 7.25 (d, J = 7.6 Hz, 1H, H-9 quinox.), 7.49 (d, J = 8.8 Hz, 1H, H-6 quinox.), 10.65 (s, 1H, SH) (D_2O exchangeable); Anal. Calcd. for $C_{11}H_{11}N_5S$ (273.36): C, 57.12; H, 5.53; N, 25.62. Found: 56.95; H, 5.75; N, 26.00.

*4.1.4. 4-([1,2,4]Triazolo[4,3-a]quinoxalin-4-ylamino)benzohydrazide (**9**)*

A mixture of the ester derivative **5** (9.5 g, 0.03 mol) and hydrazine hydrate 80% (6.0 g, 0.12 mol) in ethanol (150 ml) was stirred well and refluxed for 8 h. The solvent was evaporated and the obtained solid was faltered, washed with water several times, dried and re-crystallized from ethanol to afford the corresponding hydrazide derivative **(9)**.

Yield, 80%; m.p. 293–5 °C; IR$_{\nu max}$ (cm^{-1}): 3299, 3229 (2NH, NH2), 3054 (C—H aromatic), and 1660 (CO amide); ^{1}HNMR (400 MHz, DMSO-d_6): 4.48 (s, 2H, NH_2) (D_2O exchangeable), 7.46 (dd, J = 6.8, 8.4 Hz, 1H, H-7quinox.), 7.53 (dd, J = 7.6, 8.4 Hz, 1H, H-8 quinox.), 7.77 (d, J = 8.4 Hz, 1H, H-9 quinox.), 7.87 (dd, J = 8.8, 10 Hz, 2H, H-3 and H-5 phenyl), 8.23 (d, J = 7.6 Hz, 1H, H-6 quinox.), 8.29 (dd, J = 8.8, 10 Hz, 2H, H-2 and H-6 phenyl), 9.70 (s,1H, **NH**-NH_2) (D_2O exchangeable), 10.01(s, 1H, CH triazole), 10.53 (s,1H, **NH**-ph) (D_2O exchangeable); MS (*m/z*): 319 (M$^+$, $C_{16}H_{13}N_7O$, 18.98%), 288 (base beak, 100%), 231 (37.76%), 89 (10.02%), and 74 (31.33%); Anal. Calcd. for $C_{16}H_{13}N_7O$ (319.33): C, 60.18; H, 4.10; N, 30.70. Found: C, 60.34; H, 4.37; N, 30.97.

*4.1.5. General procedure for synthesis of target compounds (**10**$_{a,b}$)*

A mixture of the hydrazide derivative **9** (0.5 g, 0.0015 mol) and the appropriate isocyanate namely cyclohexyl and/or phenyl isocyanate (0.0022 mol) was heated under reflux in ethanol (25 ml) for 2 h. The reaction mixture was cooled and the formed solid was filtered and re-crystallized from ethanol to obtain the corresponding semicarbazides **10**$_{a,b}$ respectively.

*4.1.5.1. 2-{4-([1,2,4]Triazolo[4,3-a]quinoxalin-4-ylamino)benzoyl}-N-cyclohexylhydrazine-1-carboxamide (**10**$_a$).* Yield, 75%; m.p. 250–2 °C; IR$_{\nu max}$ (cm^{-1}): 3339, 3113 (4NH), 3067 (C—H aromatic), 2910 (C—H aliphatic), 1631 (2CO); ^{1}HNMR (400 MHz, DMSO-d_6): 1.12–1.53 (m, 6H, C-3, C-4, C-5 cyclohexyl), 1.62–1.65 (m, 2H, C-2 cyclohexyl), 1.73–1.75 (m, 2H, C-6 cyclohexyl), 3.39–3.41 (m, 1H, C-1 cyclohexyl), 6.22 (s, 1H, **NH**-cyclohexyl), 7.48 (dd, J = 7.6, 8 Hz, 1H, H-7 quinox.), 7.55 (dd, J = 7.2, 7.6 Hz, 1H, H-8 quinox.), 7.68 (s, 1H, NH of CO**N**-**H**NHCO) (D_2O exchangeable), 7.79 (d, J = 8 Hz, 1H, H-9 quinox.), 7.90 (dd, J = 8.8, 10 Hz, 2H, H-3 and H-5 phenyl), 8.25 (d, J = 7.6 Hz, 1H, H-6 quinox.), 8.30 (dd, J = 8.8, 10 Hz, 2H, H-2 and H-6 phenyl), 9.99 (s, 1H, NH of CONH**NH**CO) (D_2O exchangeable), 10.05 (s, 1H, CH triazole), 10.50 (s, 1H, **NH**-ph) (D_2O exchangeable): Anal. Calcd. for $C_{23}H_{24}N_8O2$ (440.50): C, 62.15; H, 5.44; N, 25.21. Found: C, 61.89; H, 5.63; N, 25.44.

*4.1.5.2. 2-{4-([1,2,4]Triazolo[4,3-a]quinoxalin-4-ylamino)benzoyl}-N-phenylhydrazine-1-carboxamide (**10**$_b$).* Yield, 80%; m.p. 305–7 °C; IR$_{\nu max}$ (cm^{-1}): 3277, 3174 (4NH), 3031(C—H aromatic), 1655 (2CO); ^{1}HNMR (400 MHz, DMSO-d_6): 7.15–7.19 (t, 1H, H-4′), 7.33–7.37 (m, 2H, H-3′ and H-5′), 7.47 (dd, J = 7.6, 8.4 Hz, 1H, H-7 quinox.), 7.51 (dd, J = 7.6, 8 Hz, 1H, H-8 quinox.), 7.54 (d, J = 7.6 Hz, 1H, H-9 quinox.), 7.79 (dd, J = 8.8, 9.2 Hz, 2H, H-2′ and H-6′), 8.02 (dd, J = 8, 10 Hz, 2H, H-3 and H-5 phenyl), 8.25 (d, J = 8 Hz, 1H, H-6 quinox.), 8.36 (dd, J = 8, 10 Hz, 2H, H-2 and H-6 phenyl), 9.74 (s, 1H, NH of CO**NH**NHCO) (D_2O exchangeable), 9.85 (s, 1H, NH of CONH**NH**CO) (D_2O exchangeable), 10.07 (s, 1H, CH triazolo), 10.49 (s, 1H, **NH**-ph') (D_2O exchangeable)., 10.54 (s, 1H, **NH**-ph) (D_2O exchangeable); MS (*m/z*): 438 (M$^+$, 74.38%), 339 (49.49%), 208 (45.90%), 100 (base beak, 100%), and 70 (55.57%); Anal. Calcd. for $C_{23}H_{18}N_8O_2$ (438.45): C, 63.01; H, 4.14; N, 25.56. Found: C, 63.27; H, 4.25; N, 25.73.

*4.1.6. General procedure for synthesis of target compounds (**11**$_{a-e}$)*

A mixture of the hydrazide derivative **9** (0.5 g, 0.0015 mol) and the appropriate isothiocyanate namely ethyl, propyl, butyl, cyclohexyl and/or phenyl isothiocyanate (0.0022 mol) was refluxed in ethanol (25 ml) for 6 h. The reaction mixture was cooled and the formed precipitate was filtered and re-crystallized from ethanol to obtain the corresponding thiosemicarbazides **11**$_{a-e}$ respectively.

*4.1.6.1. 2-{4-([1,2,4]Triazolo[4,3-a]quinoxalin-4-ylamino)benzoyl}-N-ethylhydrazine-1-carbothioamide (**11a**).* Yield, 80%; m.p. 250–2 °C; $IR_{\nu max}$ (cm^{-1}): 3282, 3173 (4NH), 3067 (C—H aromatic), 2977 (C—H aliphatic), 1648 (CO); ^{1}HNMR (400 MHz, DMSO-d_6): 1.08 (t, J = 7.6 Hz, 3H, CH_3), 3.50 (q, J = 7.6 Hz, 2H, CH_2), 7.48 (dd, J = 6.8, 8 Hz, 1H, H-7 quinox.),7.55 (dd, J = 7.2, 8 Hz, 1H, H-8 quinox.), 7.79 (d, J = 7.2 Hz, 1H, H-9 quinox.), 7.97 (dd, J = 8.8, 9.8 Hz, 2H, H-3 and H-5 phenyl), 8.12 (s, 1H, **NH**-CH_2-CH_3) 8.25 (d, J = 8 Hz, 1H, H-6 quinox.), 8.34 (dd, J = 8.8, 9.8 Hz, 2H, H-2 and H-6 phenyl), 9.25 (s, 1H, NH of CO**NH**NHCS) (D_2O exchangeable), 10.07 (s, 1H, CH triazolo), 10.25 (s, 1H, NH of CONH**NH**CS) (D_2O exchangeable), 10.52 (s, 1H, **NH**-ph) (D_2O exchangeable); ^{13}CNMR (100 MHz, DMSO-d_6): 26.9, 39.00, 116.67, 119.92 (2), 123.11 (2), 125.64, 126.81, 127.50, 128.13, 128.99 (2), 136.18, 138.79, 143.36, 143.40, 166.02, 181.82; Anal. Calcd. for $C_{19}H_{18}N_8OS$ (406.47): C, 56.14; H, 4.46; N, 27.57. Found: C, 56.52; H, 4.62; N, 27.41.

*4.1.6.2. 2-{4-([1,2,4]Triazolo[4,3-a]quinoxalin-4-ylamino)benzoyl}-N-propylhydrazine-1-carbothioamide (**11b**).* Yield, 85%; m.p. 255–7 °C; $IR_{\nu max}$ (cm^{-1}): 3279, 3115 (4NH), 3023 (C—H aromatic), 2907 (C—H aliphatic), 1681 (CO); ^{1}HNMR (400 MHz, DMSO-d_6): 0.85 (t, J = 7.6 Hz, 3H, CH_3) 1.54–1.57 (m, 2H, CH_2-**CH_2**-CH_3), 3.44 (t, J = 7.6 Hz, 2H, **CH_2**-CH_2-CH_3), 7.46 (dd, J = 7.2, 8 Hz, 1H, H-7 quinox.), 7.53 (dd, J = 8, 7.4 Hz, 1H, H-8of quinox.), 7.77 (d, J = 7.4 Hz, 1H, H-9 quinox.), 7.97 (dd, J = 9.2, 10.8 Hz, 2H, H-3 and H-5 phenyl), 8.12 (s, 1H, **NH**-CH_2-CH_2-CH_3) 8.23 (d, J = 7.4 Hz, 1H, H-6 quinox.), 8.34 (dd, J = 9.2, 10.8 Hz, 2H, H-2 and H-6 phenyl), 9.25 (s, 1H, NH of CO**NH**NHCS) (D_2O exchangeable), 10.05 (s, 1H, CH triazole), 10.26 (s, 1H, NH of CONH**NH**CS) (D_2O exchangeable), 10.51 (s, 1H, **NH**-ph) (D_2O exchangeable); Anal. Calcd. for $C_{20}H_{20}N_8OS$ (420.50): C, 57.13; H, 4.79; N, 26.65. Found: C, 57.46; H, 4.95; N, 26.82.

*4.1.6.3. 2-{4-([1,2,4]Triazolo[4,3-a]quinoxalin-4-ylamino)benzoyl}-N-butylhydrazine-1-carbothioamide (**11c**).* Yield, 90%; m.p. 260–2 °C; $IR_{\nu max}$ (cm^{-1}): 3279, 3100 (4NH), 3050 (C—H aromatic), 2967 (C—H aliphatic), 1657 (CO); ^{1}HNMR (400 MHz, DMSO-d_6): 0.89 (t, J = 7.6 Hz, 3H, CH_3), 1.26–1.31 (m, 2H, CH_2CH_2**CH_2**CH_3), 1.50 (m, 2H, CH_2**CH_2**CH_2CH_3), 3.46 (t, J = 7.6 Hz, 2H, **CH_2**$CH_2CH_2CH_3$), 7.51 (t, J = 8, 8.2 Hz, 1H, H-7 quinox.),7.58 (t, J = 8, 8.4 Hz, 1H, H-8 quinox.), 7.82 (d, J = 8.2 Hz, 1H, H-9 quinox.), 7.97 (dd, J = 8, 9.8 Hz, 2H, H-3 and H-5 phenyl), 8.08 (s, 1H, **NH**$CH_2CH_2CH_2CH_3$) 8.28 (d, J = 8.4 Hz, 1H, H-6 quinox.), 8.35 (dd, J = 8, 9.8 Hz, 2H, H-2 and H-6 phenyl), 9.22 (s, 1H, NH of CO**NH**NHCS) (D_2O exchangeable), 10.09 (s, 1H, CH triazolo), 10.23 (s, 1H, NH of CONH**NH**CS) (D_2O exchangeable), 10.54 (s, 1H, **NH**-ph) (D_2O exchangeable); MS (*m/z*): 434 (M^+, 8.67%), 423 (54.68%), 338 (36.51%), 312 (base beak, 100%), 278 (8.56%); Anal. Calcd. for $C_{21}H_{22}N_8OS$ (434.52): C, 58.05; H, 5.10; N, 25.79. Found: C, 58.41; H, 5.03; N, 25.92.

*4.1.6.4. 2-{4-([1,2,4]Triazolo[4,3-a]quinoxalin-4-ylamino)benzoyl}-N-cyclohexylhydrazine-1-carbothioamide (**11d**).* Yield, 85%; m.p. 265–7 °C; $IR_{\nu max}$ (cm^{-1}): 3182, 3133 (4NH), 3017 (C—H aromatic), 2900 (C—H aliphatic), 1628 (CO); ^{1}HNMR (400 MHz, DMSO-d_6): 1.23–1.56 (m, 6H, C-3, C-4, C-5 cyclohexyl), 1.64–1.68 (m, 2H, C-2 cyclohexyl), 1.75–1.78 (m, 2H, C-6 cyclohexyl), 3.39 (m, 1H, C-1 cyclohexyl), 6.27 (s, 1H, **NH**-cyclohexyl), 7.47 (dd, J = 10.8, 9.6 Hz, 1H, H-7 quinox.), 7.54 (dd, J = 6.8, 9.6 Hz, 1H, H-8 quinox.), 7.73 (s, 1H, NH of CO**NH**NHCS) (D_2O exchangeable), 7.80 (d, J = 9.6 Hz, 1H, H-9 quinox.), 7.92 (dd, J = 10, 12 Hz, 2H, H-3 and H-5 phenyl), 8.25 (d, J = 10.8 Hz, 1H, H-6 quinox.), 8.32 (dd, J = 10, 12 Hz, 2H, H-2 and H-6 phenyl), 10.02 (s, 1H, CH triazole), 10.06 (s, 1H, NH of CONH**NH**CS) (D_2O exchangeable), 10.49 (s, 1H, **NH**-ph) (D_2O exchangeable); Anal. Calcd. for $C_{23}H_{24}N_8OS$ (460.56): C, 59.98; H, 5.25; N, 24.33. Found: C, 59.87; H, 5.47; N, 24.50.

*4.1.6.5. 2-{4-([1,2,4]Triazolo[4,3-a]quinoxalin-4-ylamino)benzoyl}-N-phenylhydrazine-1-carbothioamide (**11e**).* Yield, 80%; m.p. 270–2 °C; $IR_{\nu max}$ (cm^{-1}): 3262, 3201 (4NH), 3099 (C—H aromatic), 1677 (CO); ^{1}HNMR (400 MHz, DMSO-d_6): 7.14 (t, J = 7.2 Hz, 1H, H-4 C_6H_5), 7.29–7.33 (m, 2H, H-3 and H-5 C_6H_5), 7.46 (dd, J = 7.6, 8 Hz, 1H, H-7 quinox.), 7.52 (dd, J = 7.6, 6.5 Hz, 1H, H-8 quinox.), 7.55 (d, J = 7.6 Hz, 1H, H-9 quinox.), 7.79 (dd, J = 7.2 Hz, 2H, H-2 and H-6 C_6H_5), 7.88 (dd, J = 8.8, 10 Hz, 2H, H-3 and H-5 of C_6H_4), 8.25 (d, J = 8 Hz, 1H, H-6 quinox.), 8.33 (dd, J = 8.8, 10 Hz, 2H, H-2 and H-6 C_6H_4), 9.68 (s, 1H, NH of CO**NH**NHCS) (D_2O exchangeable), 9.79 (s, 1H, NH of CONH**NH**CS) (D_2O exchangeable), 10.06 (s, 1H, CH triazole), 10.43 (s, 1H, **NH**-C_6H_4) (D_2O exchangeable), 10.52 (s, 1H, NH-C_6H_5) (D_2O exchangeable); Anal. Calcd. for $C_{23}H_{18}N_8OS$ (454.51): C, 60.78; H, 3.99; N, 24.65. Found: C, 60.51; H, 4.12; N, 24.87.

*4.1.7. General procedure for synthesis of target compounds (**12a-c**)*

A mixture of 4-Chloro-[1,2,4]triazolo[4,3-*a*]quinoxaline **4** (0.5 g, 0.002 mol) and the appropriate sulfa derivatives namely, sulfanilamide, sulfathiazole and/or sulfadiazine (0.002 mol) in the presence of few drops of TEA, was refluxed in MeCN (20 ml**)** for 10 h. The resulting precipitate was filtered, washed with *n*-hexane, air dried to obtain the target compounds **12a-c** respectively.

*4.1.7.1. 4-([1,2,4]Triazolo[4,3-a]quinoxalin-4-ylamino)benzenesulfonamide (**12a**).* Yield, 90%; m.p. 285–7 °C; $IR_{\nu max}$ (cm^{-1}): 3345, 3236 (NH, NH_2), 3106 (C—H aromatic), 1112, 1209 (SO_2); ^{1}HNMR (400 MHz, DMSO-d_6): 7.31 (s, 2H, NH_2) (D_2O exchangeable), 7.45 (dd, J = 8, 4 Hz, 1H, H-7 quinox.), 7.49 (dd, J = 8, 4 Hz, 1H, H-8 quinox.), 7.77 (d, J = 8 Hz, 1H, H-9 of quinox.), 7.85 (dd, J = 8, 7.2 Hz, 2H, H-3 and H-5 phenyl), 8.22 (d, J = 8 Hz, 1H, H-6 quinox.), 7.38 (dd, J = 8, 7.2 Hz, 2H, H-2 and H-6 phenyl), 10.04 (s, 1H, CH triazole), 10.59 (s, 1H, **NH**-ph) (D_2O exchangeable); MS (*m/z*): 340 (M^+, 22.14%), 339 (95.26%), 338 (base beak, 100%), 89 (50.13%), 75 (29.47%); Anal. Calcd. for $C_{15}H_{12}N_6O_2S$ (340.36): C, 52.93; H, 3.55; N, 24.69. Found: C, 53.18; H, 3.57; N, 24.87.

*4.1.7.2. 4-([1,2,4]Triazolo[4,3-a]quinoxalin-4-ylamino)-N-(pyrimidin-2-yl)benzenesulfonamide (**12b**).* Yield, 85%; m.p. 236–7 °C; $IR_{\nu max}$ (cm^{-1}): 3335, 3200 (2NH), 3025 (C—H aromatic), 1126, 1225 (SO_2); ^{1}HNMR (400 MHz, DMSO-d_6): 7.05 (t, J = 13.6 Hz, 1H, H-4 pyrimidine), 7.48 (dd, J = 9.6, 8.4 Hz, 1H, H-7 quinox.), 7.54 (dd, J = 8.4, 7.2 Hz, 1H, H-8 quinox.), 7.90 (d, J = 8.4 Hz, 1H, H-9 of quinox.), 8.00 (dd, J = 9.6, 10.2 Hz, 2H, H-3 and H-5 phenyl), 8.24 (d, J = 8.4 Hz, 1H, H-6 quinox.), 8.42 (dd, J = 9.6, 10.2 Hz, 2H, H-2 and H-6 phenyl), 8.51 (dd, J = 13.6 Hz, 2H, H-3 and H-5 pyrimidine), 10.8 (s, 1H, CH triazole), 10.71 (s, 1H, **NH**-ph) (D_2O exchangeable), 11.70 (s, 1H, NH of SO_2**NH**) (D_2O exchangeable); ^{13}CNMR (100 MHz, DMSO-d_6): 110.50, 114.5, 116.38 (2), 117.99 (2), 121.05, 123.74, 125.48, 125.98, 126.85 (2), 131.73, 133.81, 136.62, 142.09 (2) 155.57, 156.72; Anal. Calcd. for $C_{19}H_{14}N_8O_2S$ (418.44): C, 54.54; H, 3.37; N, 26.78. Found: C, 54.80; H, 3.54; N, 27.01.

*4.1.7.3. 4-([1,2,4]Triazolo[4,3-a]quinoxalin-4-ylamino)-N-(thiazol-2-yl) benzenesulfonamide (**12c**).* Yield, 80%; m.p. 273–5 °C; $IR_{\nu max}$ (cm^{-1}): 3300, 3250 (2NH), 3100 (C—H aromatic), 1136, 1255 (SO_2); ^{1}HNMR (400 MHz, DMSO-d_6): 6.59 (d, J = 4 Hz, 1H, H-4 of thiazole), 7.12 (d, J = 4 Hz, 1H, H-5 thiazole.), 7.43 (dd, J = 6.8, 9.6 Hz, 1H, H-7 quinox), 7.64 (dd, J = 8, 9.6 Hz, 1H, H-8 quinox.), 7.69 (d, J = 9.6 Hz, 1H, H-9 quinox.), 7.85 (dd, J = 8, 9.8 Hz, 2H, H-3 and H-5 phenyl), 8.06 (d, J = 6.8 Hz, 1H, H-6 quinox.), 8.43 (dd, J = 8, 9.8 Hz, 2H, H-2 and H-6 phenyl), 10.8 (s, 1H, CH triazole), 10.71 (s, 1H, **NH**-ph), (D_2O exchangeable), 11.70 (s, 1H, NH of SO_2**NH**) (D_2O exchangeable); MS (*m/z*): 423 (M^+, 10.07%), 342 (41.37%), 339 (base beak, 100%), 115 (27.17%); Anal. Calcd. for $C_{18}H_{13}N_7O_2S_2$ (423.47): C, 51.05; H, 3.09; N, 23.15. Found: C, 51.32; H, 3.25; N, 23.41.

*4.1.8. General procedure for synthesis of target compounds (**13$_{a,b}$**)*

The mixture of sulfonamide derivative **12$_a$** (1.0 g 0.003 mol) and anhydrous K_2CO_3 (0.82 g, 0.006 mol) in dried acetone (150 ml) was heated under reflux while stirring for 2 h, cooled, then the appropriate isocyanate namely cyclohexyl and/or phenyl isocyanate (0.0033 mol) was added. The reaction mixture was heated under reflux while stirring for 24 h. The acetone was evaporated under reduced pressure, and then water (200 ml) was added to dissolve the resulting residue. The solution was acidified with 1.0 N aqueous HCl (10 ml) and the resulting precipitate was filtered, crystallized from ethanol to yield the corresponding sulfonylurea derivatives **13$_{a,b}$** respectively.

*4.1.8.1. 4-([1,2,4]Triazolo[4,3-a]quinoxalin-4-ylamino)-N-(cyclohexylcarbamoyl)benzenesulfonamide (**13$_a$**).* Yield, 65%; m.p. 233–5 °C; $IR_{\nu max}$ (cm^{-1}): 3366 (3NH), 3087 (C—H aromatic), 2929 (C—H aliphatic), 1685 (CO), 1331, 1150 (SO_2); ^{1}HNMR (400 MHz, DMSO-d_6): 1.14–1.64 (m, 10*H*, C-2, C-3, C-4, C-5, C-6 cyclohexyl), 3.94 (m, 1H, C-1 cyclohexyl), 6.97 (s, NH, **NH**-cyclohexyl) (D_2O exchangeable), 7.13 (s, 1H, SO_2**NH**) (D_2O exchangeable), 7.53–8.42 (m, 8H, aromatic protons), 10.13 (s, 1H, CH triazolo), 10.73 (s, 1H, **NH**-ph) (D_2O exchangeable); ^{13}CNMR (100 MHz, DMSO-d_6): 25.08, 25.72, 33.49 (2), 48.59, 116.66, 120.01 (2), 123.09, 125.60, 127.06, 127.51, 128.13, 128.61 (2), 136.20, 138.74, 138.78, 143.20, 143.36, 158.12, 166.30; Anal. Calcd. for $C_{22}H_{23}N_7O_3S$ (465.53): C, 56.76; H, 4.98; N, 21.06. Found: C, 56.91; H, 4.62; N, 21.37.

*4.1.8.2. 4-([1,2,4]Triazolo[4,3-a]quinoxalin-4-ylamino)-N-(phenylcarbamoyl)benzenesulfonamide (**13$_b$**).* Yield, 85%; m.p. 245–7 °C; $IR_{\nu max}$ (cm^{-1}): 3348 (3NH), 3095 (C—H aromatic), 1685 (CO), 1327, 1149 (SO_2); ^{1}HNMR (400 MHz, DMSO-d_6): 6.55 (t, *J* = 8.8 Hz, 1H, H-4 C_6H_5), 7.13 (m, 2H, H-3 and H-5 C_6H_5), 7.27 (dd, *J* = 7.6, 8.4 Hz, 1H, H-7 quinox.), 7.34 (dd, *J* = 7.6, 8 Hz, 1H, H-8 quinox.), 7.44 (d, *J* = 7.6 Hz, 1H, H-9 quinox.), 7.53 (dd, *J* = 8, 8 Hz, 2H, H-2 and H-6 C_6H_5), 7.95 (dd, *J* = 8.4, 9.2 Hz, 2H, H-2 and H-6 C_6H_4), 8.28 (d, *J* = 8 Hz, 1H, H-6 quinox.), 8.47 (dd, *J* = 8.4, 9.2 Hz, 2H, H-3 and H-5 C_6H_4), 8.88 (s, 1H, NH of ph-SO_2**NH**) (D_2O exchangeable), 10.08 (s, 1H, CH triazole), 10.62 (s, 1H, **NH**-C_6H_4) (D_2O exchangeable), 10.76 (s, 1H, NH of —CO**NH**-C_6H_5) (D_2O exchangeable); ^{13}CNMR (100 MHz, DMSO-d_6): 116.67, 117.74, 120.50 (2), 123.15, 125.25, 126.85 (2), 127.55, 128.12, 128.53, 136.11, 136.36, 138.20, 138.75, 138.79, 141.01, 141.82, 142.88, 143.23, 143.39,159.34; MS (*m/z*): 459 (M^+, 8.91%), 424 (34.17%), 341 (base beak, 100%), 305 (39.58%) 90 (43.27%); Anal. Calcd. for $C_{22}H_{17}N_7O_3S$ (459.48): C, 57.51; H, 3.73; N, 21.34. Found: C, 57.83; H, 3.86; N, 21.52.

*4.1.9. General procedure for synthesis of target compounds (**14$_{a-d}$**)*

A mixture of sulfonamide derivative **12$_a$** (1.0 g, 0.003 mol) and anhydrous K2CO3(0.82 g, 0.006 mol) in dried acetone (150 ml) was heated under reflux while stirring for 2 h, cooled, then the appropriate isothiocyanate namely ethyl, propyl, butyl and/or phenyl isothiocyanate (0.0033 mol) was added to the reaction mixture. Refluxing and stirring were continued for 24 h. The acetone was evaporated under reduced pressure, and then water (200 ml) was added to dissolve the resulting residue. The solution was acidified with 1.0 N aqueous HCl (10 ml) and the resulting precipitate was filtered and crystallized from ethanol to yield the corresponding sulfonylthiourea derivatives **14$_{a-e}$** respectively.

*4.1.9.1. 4-([1,2,4]Triazolo[4,3-a]quinoxalin-4-ylamino)-N-(ethylcarbamothioyl)benzenesulfonamide (**14$_a$**).* Yield, 60%; m.p. 222–4 °C; $IR_{\nu max}$ (cm^{-1}): 3340 (3NH), 3087 (C—H aromatic), 2944 (C—H aliphatic), 1682 (CO), 1383, 1148 (SO_2); ^{1}HNMR (400 MHz, DMSO-d_6): 1.05 (t, *J* = 10.4 Hz, 3H, CH_3), 3.40 (q, *J* = 10.4 Hz, 2H, CH_2), 7.50 (dd, *J* = 11.2, 6.8 Hz, 1H, H-7 quinox.), 7.54 (dd, *J* = 10.4, 6.8 Hz, 1H, H-8 quinox.), 7.61 (d, *J* = 6.8 Hz, 1H, H-9 quinox.), 7.84 (dd, *J* = 8, 9.2 Hz, 2H, H-3 and H-5 phenyl), 7.93 (s, 1H, **NH**-CH_2-CH_3) 8.27 (d, *J* = 6.8 Hz, 1H, H-6 quinox.), 8.46 (dd, *J* = 8, 9.2 Hz, 2H, H-2 and H-6 phenyl), 10.09 (s, 1H, CH triazolo), 10.77 (s, 1H, **NH**-ph) (D_2O exchangeable), 11.39 (s, 1H, NH of SO_2**NH**CS) (D_2O exchangeable); Anal. Calcd. for $C_{18}H_{17}N_7O_2S_2$ (427.50): C, 50.57; H, 4.01; N, 22.94. Found: C, 50.34; H, 4.24; N, 23.17.

*4.1.9.2. 4-([1,2,4]Triazolo[4,3-a]quinoxalin-4-ylamino)-N-(propylcarbamothioyl)benzenesulfonamide (**14$_b$**).* Yield, 85%; m.p. 227–9 °C; $IR_{\nu max}$ (cm^{-1}): 3330 (3NH), 3037 (C—H aromatic), 2999 (C—H aliphatic), 1662 (CO), 1350, 1198 (SO_2); ^{1}HNMR (400 MHz, DMSO-d_6): 0.85 (t, *J* = 10.4 Hz, 3H, CH_3), 1.47–1.51 (m, 2H, CH_2**CH_2**CH_3), 3.45 (q, *J* = 10.4 Hz, 2H, **CH_2**CH_2CH_3) 7.50 (dd, *J* = 11.2, 6.8 Hz, 1H, H-7 quinox.),7.55 (dd, *J* = 10.4, 6.8 Hz, 1H, H-8 quinox.), 7.61 (d, *J* = 6.8 Hz, 1H, H-9 quinox.), 7.79 (dd, *J* = 8, 10.2 Hz, 2H, H-3 and H-5 phenyl), 7.95 (s, 1H, **NH**-CH_2-CH_2-CH_3) 8.25 (d, *J* = 6.8 Hz, 1H, H-6 quinox.), 8.46 (dd, *J* = 8, 10.2 Hz, 2H, H-2 and H-6 phenyl), 10.06 (s, 1H, CH triazole), 10.75 (s, 1H, **NH**-ph) (D_2O exchangeable), 11.45 (s, 1H, NH of SO_2**NH**CS) (D_2O exchangeable); ^{13}CNMR (100 MHz, DMSO-d_6): 11.60, 21.48, 46.69, 116.72, 120.27 (2), 123.27, 126.04, 127.71, 128.17, 128.77 (2), 132.52, 135.92, 138.80, 143.26, 144.89, 166.02, 178.53; Anal. Calcd. for $C_{19}H_{19}N_7O_2S_2$ (441.53): C, 51.69; H, 4.34; N, 22.21. Found: C, 51.98; H, 4.19; N, 22.57.

*4.1.9.3. 4-([1,2,4]Triazolo[4,3-a]quinoxalin-4-ylamino)-N-(butylcarbamothioyl)benzenesulfonamide (**14$_c$**).* Yield, 70%; m.p. 233–5 °C; $IR_{\nu max}$ (cm^{-1}): 3300 (3NH), 3080 (C—H aromatic), 2895 (C—H aliphatic), 1680 (CO amide), 1303, 1171 (SO_2); ^{1}HNMR (400 MHz, DMSO-d_6): 0.84 (t, *J* = 10.4 Hz, 3H, CH_3), 1.26 (m, 2H, CH_2-CH_2**CH_2**CH_3), 1.35–1.46 (m, 2H, CH_2**CH_2**CH_2CH_3), 3.13 (q, *J* = 10.4 Hz, 2H, **CH_2**$CH_2CH_2CH_3$), 7.58 (dd, *J* = 7.2, 8.8 Hz, 1H, H-7 of quinox.), 7.63 (dd, *J* = 7.2, 8.8 Hz, 1H, H-8 quinox.), 7.69 (d, *J* = 7.2 Hz, 1H, H-9 quinox.), 7.90 (dd, *J* = 8.4, 10.2 Hz, 2H, H-3 and H-5 phenyl), 7.93 (s, 1H, **NH**-$CH_2CH_2CH_2CH_3$) 8.27 (d, *J* = 7.2 Hz, 1H, H-6 quinox.), 8.47 (dd, *J* = 8.4, 10.2 Hz, 2H, H-2 and H-6 phenyl), 10.09 (s, 1H, CH triazole), 10.74 (s, 1H, **NH**-ph) (D_2O exchangeable), 11.43 (s, 1H, NH of SO_2**NH**CS) (D_2O exchangeable); Anal. Calcd. for $C_{20}H_{21}N_7O_2S_2$ (455.56): C, 52.73; H, 4.65; N, 21.52. Found: C, 52.97; H, 4.78; N, 21.80.

*4.1.9.4. 4-([1,2,4]Triazolo[4,3-a]quinoxalin-4-ylamino)-N-(phenylcarbamothioyl)benzenesulfonamide (**14$_d$**).* Yield, 70%; m.p. 240–2 °C; $IR_{\nu max}$ (cm^{-1}): 3299 (3NH), 3077 (C—H aromatic), 2900 (C—H aliphatic), 1672 (CO amide), 1343, 1118 (SO_2); ^{1}HNMR (400 MHz, DMSO-d_6): 6.92 (t, *J* = 7.2 Hz, 1H, H-4 C_6H_5), 7.03–7.25 (m, 2H, H-3 and H-5 C_6H_5), 7.26 (dd, *J* = 7.6, 8.4 Hz, 1H, H-7 quinox.), 7.35 (dd, *J* = 7.6, 8 Hz, 1H, H-8 quinox.), 7.46 (d, *J* = 7.6 Hz, 1H, H-9 quinox.), 7.55 (dd, *J* = 7.2 Hz, 2H, H-2 and H-6 C_6H_5), 7.83 (dd, *J* = 8.4, 10 Hz, 2H, H-2 and H-6 C_6H_4), 8.28 (d, *J* = 8 Hz, 1H, H-6 quinox.), 8.47 (dd, *J* = 8.4, 10 Hz, 2H, H-3 and H-5 C_6H_4), 8.97 (s, 1H, NH of ph-SO_2**NH**CS) (D_2O exchangeable), 10.08 (s, 1H, CH triazole), 10.65 (s, 1H, **NH**-C_6H_4) (D_2O exchangeable), 10.78 (s, 1H, NH of -CS**NH**-C_6H_5) (D_2O exchangeable); Anal. Calcd. for $C_{22}H_{17}N_7O_2S_2$ (475.55): C, 55.57; H, 3.60; N, 20.62. Found: C, 55.38; H, 3.86; N, 20.43.

4.2. Docking studies

In the present work, all the target compounds were subjected to docking study to explore their binding mode towards DNA-Top II. All modeling experiments were performed using molsoft program, which provides a unique set of tools for the modeling of protein/ligand interactions. It predicts how small flexible molecule such as substrates or drug candidates bind to a protein of known 3D structure represented by grid interaction potentials (http://www.molsoft.com/icm_pro.html). Each experiment used the biological target DNA-Top II downloaded from the Brookhaven Protein Databank (http://www.rcsb.org/pdb/ex

plore/explore.do?structureId = 4G0U). In order to qualify the docking results in terms of accuracy of the predicted binding conformations in comparison with the experimental procedure, the reported DNA-Top II inhibitor drug doxorubicin was used as reference ligand.

4.3. In vitro anti-proliferative activity

The cytotoxicity assays were performed at Pharmacology & Toxicology Department, Faculty of pharmacy, Al-Azhar University, Cairo, Egypt. Cancer cells from different cancer cell lines hepatocellular carcinoma (HepG2), colorectal carcinoma (HCT-116) and breast cancer (MCF-7), were purchased from American type Cell Culture collection (ATCC, Manassas, USA) and grown on the appropriate growth medium Roswell Park Memorial Institute medium (RPMI 1640) supplemented with 100 mg/mL of streptomycin, 100 units/mL of penicillin and 10% of heat-inactivated fetal bovine serum in a humidified, 5% (v/v) CO_2 atmosphere at 37 °C Cytotoxicity assay by 3-[4,5-dimethylthiazole-2-yl]-2,5-diphenyltetrazolium bromide (MTT).

Exponentially growing cells from different cancer cell lines were trypsinized, counted and seeded at the appropriate densities (2000–1000 cells/0.33 cm2 well) into 96-well microtiter plates. Cells then were incubated in a humidified atmosphere at 37C for 24 h. Then, cells were exposed to different concentrations of compounds (0.1, 10, 100 and 1000 μM) for 72 h. Then the viability of treated cells was determined using MTT technique as follow. Cells were incubated with 200 μl of 5% MTT solution/well (Sigma Aldrich, MO) and were allowed to metabolize the dye into colored-insoluble formazan crystals for 2 h. The remaining MTT solution were discarded from the wells and the formazan crystals were dissolved in 200 μl/well acidified isopropanol for 30 min, covered with aluminum foil and with continuous shaking using a MaxQ 2000 plate shaker (Thermo Fisher Scientific Inc, MI) at room temperature. The colorimetric assay was measured and recorded at absorbance of 570 nm using a Stat FaxR 4200 plate reader (Awareness Technology, Inc., FL). The cell viability were expressed as percentage of control and the concentration that induces 50% of maximum inhibition of cell proliferation (IC_{50}) were determined using Graph Pad Prism version 5 software (Graph Pad software Inc, CA) [42–44].

4.3.1. In vitro DNA/Methyl green assay

Fourteen compounds exhibited significant anti-proliferative activities (**8_{a-e}, $10_{a,b}$, 11_{b-e}, 13_a** and **$14_{b,c}$**) were further evaluated to determine their DNA-binding affinities. Doxorubicin as DNA intercalator was used as positive control. In this test, methyl green dye can bind DNA to form colored reversible complex of DNA/methyl green. These complexes still stable at neutral pH. Upon addition of intercalating agents, the methyl green is displaced from DNA with addition of H_2O molecule to the dye resulting in formation of the colorless carbinol, leading to a dramatic decrease in spectrophotometric absorbance [20,21,45]. ΔA value (the difference between DNA/methyl green complex and free cabinol) provides the simplest means for detecting the DNA-binding affinity and relative binding strength. IC_{50} values were determined using the GraphPadPrism 5.0 software. The reaction was performed as follows.

A mixture of Calf thymus DNA (10 mg) and methyl green (20 mg) (Sigma–Aldrich) in 100 ml of 0.05 M Tris-HCl buffer (pH 7.5) containing 7.5 mM $MgSO_4$. Then,the mixture was stirred for 24 h at 37 °C. The test samples were dissolved in ethanol and dispensed into wells of a 96-well microtiter tray at concentration of 10,100 and 1000 μM. From each well, the excess solvent was removed under vacuum followed by addition of 200 μl of the DNA/methyl green solution. The test samples were incubated in a dark at ambient temperature. After 24 h, the absorbance of each sample was determined at 642.5–645 nm. Readings were corrected for initial absorbance and normalized as the percentage of the untreated DNA/methyl green absorbance value.

4.3.2. In vitro Topoisomerase II inhibitory activity

Six compounds showed high anti-proliferative and DNA-binding activities (**8_a, 8_b, 8_c, 8_e, 10_a** and **11_d**) were further evaluated to assess their Topo II inhibitory activities. In this test, Topo II drug screening kit (TopoGEN, Inc., Columbus) was utilized to determine the Topo II activity according to the reported method [20]. Doxorubicin was used as a reference drug in this test.

A typical enzyme reaction contained a mixture of human Topo II (2 μl), substrate super coiled pHot1 DNA (0.25 μg), 50 μg/ml test compound (2 μl), and assay buffer (4 μl). The reaction started upon incubation of the mixture in 37 °C for 30 min. The reaction was terminated by addition of 10% sodium dodecylsulphate (2 μl) and proteinase K (50 μg/ml) at 37 °C for 15 min. followed by incubation for 15 min at 37 °C. Then, the DNA was run on 1% agarose gel in BioRad gel electrophoresis system for 1–2 h followed by staining with GelRedTM stain for 2 h and destained for 15 min with TAE buffer. The gel was imaged via BioRad's Gel DocTMEZ system. Both supercoiled and linear strands DNA were incorporated in the gel as markers for DNA-Topo II intercalators. The results of IC_{50} values were calculated using the GraphPad Prism version 5.0. Each reaction was performed in duplicate, and at least three independent determinations of each IC_{50} were made.

Declaration of Competing Interest

The authors declare that they have no known competing financial interests or personal relationships that could have appeared to influence the work reported in this paper.

Acknowledgement

The authors extend their appreciation and thanking to Dr. Tamer Abdel-Ghany, Pharmacology & Toxicology Department, Faculty of Pharmacy, Al-Azhar University, Cairo, Egypt for helping in the pharmacological part.

Appendix A. Supplementary material

Supplementary data to this article can be found online at https://doi.org/10.1016/j.bioorg.2020.104399.

References

[1] B.A. Armitage, Cyanine dye–DNA interactions: intercalation, groove binding, and aggregation, in: DNA binders and related subjects, Springer, 2005, pp. 55–76.
[2] Y. Pommier, E. Leo, HongLiang Zhang, C. Marchand, DNA topoisomerases and their poisoning by anticancer and antibacterial drugs, Chem. Biol. 17 (5) (2010) 421–433.
[3] J.L. Nitiss, Targeting DNA topoisomerase II in cancer chemotherapy, Nat. Rev. Cancer 9 (5) (2009) 338–350.
[4] L. Strekowski, B. Wilson, Noncovalent interactions with DNA: an overview, Mutation Res. 623 (1-2) (2007) 3–13.
[5] A. Paul, S. Bhattacharya, Chemistry and biology of DNA-binding small molecules, Curr. Sci. 102 (2012) 212–231.
[6] S. Kumar, et al., Structural studies on ligand—DNA system. A rubst approach in drug design, J. of Biosci. 37 (2012) 553–561.
[7] R. Palchaudhuri, P.J. Hergenrother, DNA as a target for anticancer compounds: methods to determine the mode of binding and the mechanism of action, Curr. Opin. Biotechnol. 18 (6) (2007) 497–503.
[8] C.F. Guerra, F.M. Bickelhaupt, WatsonCrick hydrogen bonds: nature and role in DNA replication, Modern Meth. Theor. Phys. Chem. Biopolym. 19 (2006) 79–97.
[9] N. Langkjær, J. Wengel, A. Pasternak, Watson–Crick hydrogen bonding of unlocked nucleic acids, Bioorg. Medi. Chem. Lett. 25 (22) (2015) 5064–5066.
[10] H. Lodish, et al., The Role of topoisomerases in DNA replication, Molecular Cell Biology, fourth ed., Section 12.3, 2000, Available from: https://www.ncbi.nlm.nih.gov/books/NBK21703/ (accessed April 2018).
[11] W.A. Denny, Emerging DNA topoisomerase inhibitors as anticancer drugs, Expert Opin. Emerg. Drugs 9 (1) (2004) 105–133.
[12] M.A. Hogan, D.S. McKinney, Comprehensive Review for NCLEX-PN, second ed., Pearson, 2012.
[13] J.L. Delgado, et al., Topoisomerases as anticancer targets, Biochem J. 475 (2) (2018) 373–398, https://doi.org/10.1042/BCJ20160583. PMID: 29363591; PMCID: PMC6110615.

[14] R. Martinez, L. Chacon-Garcia, The search of DNA-intercalators as antitumoral drugs: what it worked and what did not work, Curr. Med. Chem. 12 (2005) 127–151.
[15] L.F. Liu, DNA topoisomerase poisons as antitumor drugs, Annu. Rev. Biochem. 58 (1) (1989) 351–375.
[16] A. Chilin, G. Marzaro, C. Marzano, L.D. Via, M.G. Ferlin, G. Pastorini, A. Guiotto, Synthesis and antitumor activity of novel amsacrine analogs: the critical role of the acridine moiety in determining their biological activity, Bioorg. Med. Chem. 17 (2) (2009) 523–529.
[17] T.D. Shenkenberg, D.D. Von Hoff, Mitoxantrone: a new anticancer drug with significant clinical activity, Ann. Intern. Med. 105 (1986) 67–81.
[18] C. Avendano, J. Menéndez, DNA Intercalators and topoisomerase inhibitors, in: Medicinal Chemistry of Anticancer Drugs, second ed., Elsevier, 2008, pp. 199–228.
[19] Y.C. Liaw, Y.G. Gao, H. Robinson, G.A. Van der Marel, J.H. Van Boom, A.H. J. Wang, Antitumor drug nogalamycin binds DNA in both grooves simultaneously: molecular structure of nogalamycin-DNA complex, Biochemistry 28 (26) (1989) 9913–9918.
[20] I.H. Eissa, et al., Discovery and antiproliferative evaluation of new quinoxalines as potential DNA intercalators and topoisomerase II inhibitors, Archiv der Pharmazie 352 (11) (2019), e1900123, https://doi.org/10.1002/ardp.201900123.
[21] M.-K. Ibrahim, et al., Design, synthesis, molecular modeling and anti-proliferative evaluation of novel quinoxaline derivatives as potential DNA intercalators and topoisomerase II inhibitors, Eur. J. Med. Chem. 155 (2018) 117–134, https://doi.org/10.1016/j.ejmech.2018.06.004.
[22] I.H. Eissa, et al., Design and discovery of novel quinoxaline derivatives as dual DNA intercalators and topoisomerase II inhibitors, Anticancer Agents Med. Chem. 18 (2) (2018) 195–209, https://doi.org/10.2174/1871520617666170710182405.
[23] T. Mahata, et al., The benzyl moiety in a quinoxaline-based scaffold acts as a DNA intercalation switch, Angew. Chem. Int. Ed. 55 (2016) 7733–7736.
[24] B. Oyallon, et al., Structure-based design of novel quinoxaline-2-carboxylic acids and analogues as Pim-1 inhibitors, Eur. J. Med. Chem. 154 (2018) 101–109.
[25] M.G. Varrica, et al., DNA intercalators based on (1, 10-phenanthrolin-2-yl) isoxazolidin-5-yl core with better growth inhibition and selectivity than cisplatin upon head and neck squamous cells carcinoma, Eur. J. Med. Chem. 143 (2018) 583–590.
[26] Y.-S. Park, et al., Molecular and cellular toxicological profiling of DNA bis-intercalator, quinoxaline compounds: echinomycin as the versatile lead, J. Biochem. Mol. Toxicol. 14 (2018) 9–18.
[27] K. El-Adl, et al., 5-(4-Methoxybenzylidene)thiazolidine-2,4-dione-derived VEGFR-2 inhibitors: design, synthesis, molecular docking, and anticancer evaluations, Arch Pharm. 353 (9) (2020), e2000079, https://doi.org/10.1002/ardp.202000079.
[28] K. El-Adl, et al., Design, synthesis, molecular docking, and anticancer evaluations of 1-benzylquinazoline-2,4(1*H*,3*H*)-dione bearing different moieties as VEGFR-2 inhibitors, Arch. Pharm. 353 (8) (2020), e2000068, https://doi.org/10.1002/ardp.202000068.
[29] K. El-Adl, et al., Design, synthesis, molecular docking and anticancer evaluations of 5-benzylidenethiazolidine-2,4-dione derivatives targeting VEGFR-2 enzyme, Bioorg. Chem. 102 (2020), 104059, https://doi.org/10.1016/j.bioorg.2020.104059. Epub 2020 Jun 30 PMID: 32653608.
[30] A.G.A. El-Helby, et al., Benzoxazole/benzothiazole-derived VEGFR-2 inhibitors: design, synthesis, molecular docking, and anticancer evaluations, Archiv der Pharmazie 352 (12) (2019), e1900178, https://doi.org/10.1002/ardp.201900178. Epub 2019 Oct 9 PMID: 31596514.
[31] A.G.A. El-Helby, et al., Design, synthesis, molecular docking, and anticancer activity of benzoxazole derivatives as VEGFR-2 inhibitors, Archiv der Pharmazie 352 (10) (2019), e1900113, https://doi.org/10.1002/ardp.201900113. PMID: 31448458.
[32] A.G.A. El-Helby, et al., Design, synthesis, in vitro anti-cancer activity, ADMET profile and molecular docking of novel triazolo [3, 4-a] phthalazine derivatives targeting VEGFR-2 enzyme, Anti-Cancer Agents Med. Chem. (Formerly Current Medicinal Chemistry-Anti-Cancer Agents) 18 (8) (2018) 1184–1196.
[33] A.G.A. El-Helby, et al., Design, synthesis, molecular docking, and anticancer activity of phthalazine derivatives as VEGFR-2 Inhibitors, Archiv der Pharmazie 350 (12) (2017), https://doi.org/10.1002/ardp.201700240. Epub 2017 Nov 13. PMID: 29131379.
[34] D.E. Graves, L.M. Velea, Intercalative binding of small molecules to nucleic acids, Curr. Org. Chem. 4 (2000) 915–929.
[35] F. Gago, Stacking interactions and intercalative DNA binding, Methods 14 (1998) 277–292.
[36] G. Minotti, et al., Anthracyclines: molecular advances and pharmacologic developments in antitumor activity and cardiotoxicity, Pharmacol. Rev. 56 (2004) 185–229.
[37] J. Gallego, et al., Structure–affinity relationships for the binding of actinomycin D to DNA, J. Comput. Aided Mol. Des. 11 (1997) 114–128.
[38] S.A. Bailey, et al., Binding of actinomycin D to the T (G) nT motif of double-stranded DNA: determination of the guanine requirement in nonclassical, non-GpC binding sites, Biochemistry 33 (1994) 11493–11500.
[39] M. Alswah, et al., Design, synthesis and cytotoxic evaluation of novel chalcone derivatives bearing triazolo[4,3-a]-quinoxaline Moieties as potent anticancer agents with dual EGFR kinase and tubulin polymerization inhibitory effects, Molecules 23 (1) (2017) 48–63, https://doi.org/10.3390/molecules23010048.
[40] A.M. Soliman, A.A. Amer, Synthesis and antimicrobial activity of some novel quinoxalines, Synthetic Commun: Int. J. Rapid Commun. Synthetic Org. Chem. 42 (10) (2012) 1401–1410, https://doi.org/10.1080/00397911.2010.537802.
[41] C.C. Wu, et al., Structural basis of type II topoisomerase inhibition by the anticancer drug etoposide, Science 333 (6041) (2011) 459–462, https://doi.org/10.1126/science.1204117.
[42] K. Mena-Ulecia, et al., Study of the differential activity of thrombin inhibitors using docking, QSAR, molecular dynamics, and MM-GBSA, PLoS One 10 (11) (2015), e0142774, https://doi.org/10.1371/journal.pone.0142774. PMID: 26599107; PMCID: PMC4657979.
[43] T. Mosmann, Rapid colorimetric assay for cellular growth and survival: application to proliferation and cytotoxicity assays, J. Immunol. Methods 65 (1–2) (1983) 55–63.
[44] D.A. Scudiero, et al., Evaluation of a soluble tetrazolium/formazan assay for cell growth and drug sensitivity in culture using human and other tumor cell lines, Cancer Res. 48 (17) (1988) 4827–4833.
[45] F.M. Freimoser, C.A. Jakob, M. Aebi, U. Tuor, The MTT [3-(4,5-dimethylthiazol-2-yl)-2,5-diphenyltetrazolium bromide] assay is a fast and reliable method for colorimetric determination of fungal cell densities, Appl. Environ. Microbiol. 65 (8) (1999) 3727–3729.
[46] N.S. Burres, et al., A colorimetric microassay for the detection of agents that interact with DNA, J. Nat. Prod. 55 (1992) 1582–1587.